STRATIGRAPHIC AND STRUCTURAL INTERPRETATION OF SEISMIC SECTIONS IN LOKICHAR BASIN

By:

ANABWANI JOSKY KISALI

I56/63948/2010

A DISSERTATION

SUBMITTED IN PARTIAL FULFILLMENT FOR THE AWARD OF MASTERS OF SCIENCE GEOLOGY DEGREE

(APPLIED GEOPHYSICS)

AUGUST 2012

UNIVERSITY OF NAIROBI

Declaration

I declare that the work contained in this dissertation is my original work and has not been submitted for a degree at any other University. To the best of my knowledge, the dissertation contains no material previously published or written by other authors except where due reference is made.

Signed ………………………………….. Date ………………………………………..

ANABWANI JOSKY KISALI

This dissertation has been submitted for examination with our knowledge as the University Supervisors.

Signed……………………………………… Date ………………………………………..

PROF. JUSTUS O. BARONGO

DEPARTMENTOF GEOLOGY, UNIVERSITY OF NAIROBI

Signed……………………………………… Date ………………………………………..

DR. JOSPHAT K. MULWA

DEPARTMENTOF GEOLOGY, UNIVERSITY OF NAIROBI

Abstract

This research was carried out in Lokichar Basin located in Turkana County in Northwestern Kenya. The study area is within the Tertiary Rift Basin of the four sedimentary basins of Kenya which include Lamu, Anza, Mandera and Tertiary Rift basins. Lokichar basin consists of relatively simple structural geometry with a major basin-bounding fault on the western margin called Lokichar fault, and a flexural margin on the eastern margin.

The present investigation involved the interpretation of old secondary seismic sections in order to come up with a subsurface structure with an aim of identifying and delineating possible hydrocarbon traps and prospective areas. Five lines of 2D seismic data from Lokichar basin were interpreted. Data analysis and interpretation was done using SMT Kingdom Suite vers 8.6 software. The interpretation process involved picking and tracing of horizons and faults of interest from the vertical seismic displays of the seismic lines.

Interpreted results have confirmed that there exists a major bounding fault called Lokichar fault on the western side of the basin. The fault could be responsible for controlling sediments deposition within Lokichar basin. Lokichar fault was determined to be generally a normal low angle fault that dips towards the east. Similarly, most of the other faults interpreted were found to be mostly high angle, listric in nature and generally dipping towards the east.

Positive and negative flower structures were found to be common in Lokichar basin. Structures that control hydrocarbon accumulation and trapping were identified to be fault closures and fold anticlines. These structures could therefore form the target areas for hydrocarbon prospecting. On the interpreted seismic lines, hydrocarbon prospective areas were estimated based on the results of Loperot-1 well.

Dedication

This dissertation is dedicated to the Almighty God for His grace and for giving me strength. It is also dedicated to my parents, relatives and friends for their continued encouragement and guidance. Lastly in memory of my late grandfather who was very instrumental to me throughout his lifetime.

Acknowledgement

I would like to thank Prof J.O. Barongo for his continued assistance and guidance during this research work. He also provided the software to carry out the research. I acknowledge Dr. J. K. Mulwa for his very contributive assistance and guidance throughout this research work.

NOCK provided the data geological reports and maps necessary for this research work. I am extremely grateful to NOCK for its generosity without which this dissertation would not have been possible. Credit goes to Mr. Edmond Makhanu a geophysicist at NOCK who was very helpful in providing the data set used in this research. He also provided technical support in regard to working with seismic data which was very helpful in completion of this research.

Great thanks to all the Master of Science (Geology) 2010 class especially Charity Cheruiyot, Junior Kimata, Philip Omollo, Gregory Odawo and Dhieu Ater for their contribution and ideas. I am very grateful to all my colleagues at Ministry of Energy Kenya and department of Geology University of Nairobi who made this research work possible.

Finally I would like to thank the Ministry of Energy Kenya for offering me a scholarship and financial support to study Master of Science (Geology) degree at the University of Nairobi.

Table of contents

List of Figures

List of Abbreviations

2D: Two dimensional

3D: Three dimensional

HI: Hydrogen Index

KRISP: Kenya Rift International Seismic Project

Ma: Million years

NOCK: National Oil Corporation of Kenya

rms: root mean square

SEGY: Society of Exploration Geophysicists Y-format

SMT: Seismic Micro Technology

SP: Shot Point

TWT: Two way traveltime

CHAPTER ONE

1.0. INTRODUCTION

The Tertiary rift has attracted a lot of interest in the exploration of hydrocarbon and geothermal resources and expanded the understanding of subsurface structures, stratigraphy, and petrology of the basin (Feibel 2011). This research was carried out in Lokichar Basin located within the Tertiary rift to the south-southwest of the N-S trending part of Lake Turkana as shown in Figure 1-1.

Lokichar Basin is a N-S-trending, east-facing half-graben, 60 km long and 30 km wide and floored by Precambrian crystalline basement (Tiercelin et al., 2009). The Basin contains up to 7 km of Paleogene to Miocene age rocks (Vitel et al., 2004). It has a relatively simple structural geometry with a major basin-bounding fault on the western margin called Lokichar fault (Figure 2-2), and a flexural margin on the eastern margin.

The Tertiary rift contain transfer zones which are important features in understanding the distribution of hydrocarbons since they not only make changes in large scale structural style but can also contain structures different from other parts (Morley 1995). Transfer zones are sites where boundary faults die out, uplift becomes less severe and major topographic breaks occur providing entry point for large fluvial systems into the rift basin (Ray and Mayor 2006).

The present investigation involved interpretation of 5 lines of 2D seismic data within Lokichar basin with the aim of understanding and determining sub-surface structures and possible hydrocarbon prospective areas. The area of study has indications of hydrocarbons based on the results of Loperot-1 well where the well encountered source rocks and reservoirs bearing oil.

Data available to carry out this research was old secondary data acquired by Amoco Kenya Company in 1985. The data was provided by NOCK. Interpretations of the seismic lines were done using SMT kingdom Suite ver 8.6 interpretation software. These seismic lines were chosen based on the availability of data in digital form since tapes for most of the lines from the region were not available. Therefore most seismic lines available from the area do not have digital data.

Seismic data is analyzed in order to produce a model of the (unseen) subsurface (Admasu 2008). This analysis (or the interpretation) encompasses different stages where underground rock layer properties are identified. Results from analysis are crucial for reservoir prospect evaluation and hence influence the subsequent economic viability (Admasu 2008). Seismic interpretation provides an assessment of a prospect's hydrocarbon potential and, if favorable, identify best locations for drilling wells (Gadallah & Fisher 2009). Interpretations can be obtained manually, by signal consistent automatic extraction of minimum, maximum or zero crossing surfaces, or by combining automated surface extraction with manual interpretation (Borgos et al., 2005).

Geophysical methods, mainly seismic methods, are used to map out sedimentary basins on a regional scale and also on a small scale for detailed exploration and production (Bjorlykke 2010). The major goal of seismic interpretation is to relate surface-acquired reflection seismic data to subsurface stratigraphy and depositional facies (Gadallah & Fisher 2009).

1.1. Statement of the problem

Since the study area is within a rift system, hydrocarbon occurrence and distribution in the rift is largely a product of the stratigraphic succession in the syn- and post-rift phases of the basin evolution. Most of the known recoverable hydrocarbon reserves occur in rifts with post-rift sag basins and in those basins that are dominated by marine fill (Lambiase et al., 1999). Rifts contain transfer zones which are important features in understanding the distribution of hydrocarbons since they not only make changes in large scale structural style but can also contain structures different from other parts (Morley 1995).

Following the recent discoveries of a major oil field in the Albertine Graben in Uganda and two gas fields of Songo Songo and Mnazi bay in the Ruvuma and Rufiji basins of Tanzania, respectively, it is evident that all the basins of East Africa display good source rocks capable of generating oil and gas, together with good to excellent reservoir rocks and structures conducive for the accumulation of oil and gas (Thuo 2009).

Lokichar basin has attracted a lot of research by oil companies with the intention of discovering commercial reserves of hydrocarbons but most of their findings are not in the public domain. Only activity reports of oil companies with little technical information are available. Rapid increasing demand for oil and gas worldwide has caused an increase in exploration in pre-explored and un-explored areas around the world such as the Lokichar basin area. Therefore, the oil industry is constantly looking for better data acquisition and processing methods (Admasu 2008).

The purpose of this research was to come up with structural information that will be available to the public domain to be used by other researchers. It is evident from literature review that most previous studies on the area were mostly focused on the evolution and morphology of the rift and very little is known on how seismic data is interpreted and results modeled for the purpose of identifying strata and structures that could possibly lead to the determination of hydrocarbon occurrence. The Tertiary rift system in Kenya is a capable reserve for hydrocarbons if detailed exploration and accurate interpretation of previous data and new data is carried out.

1.2. The study area

1.2.1. Location

Lokichar basin is located in Turkana County within the Tertiary rift in the northwestern part of Kenya to the southwest of Lake Turkana. It is bound by longitudes $35^o30'$E and $36^o20'$E and latitudes $2^o00'$N and $3^o00'$N (Figure 1-1). The basin is 30 km wide and 60 km long in dimension (area≈1200 km$^{2)}$. The study area is thinly populated with tarmac roads for good access from major towns to Lodwar (Figure 1-1 and 1-3), but within the basin, there are very scarce and poor roads and telecommunication facilities.

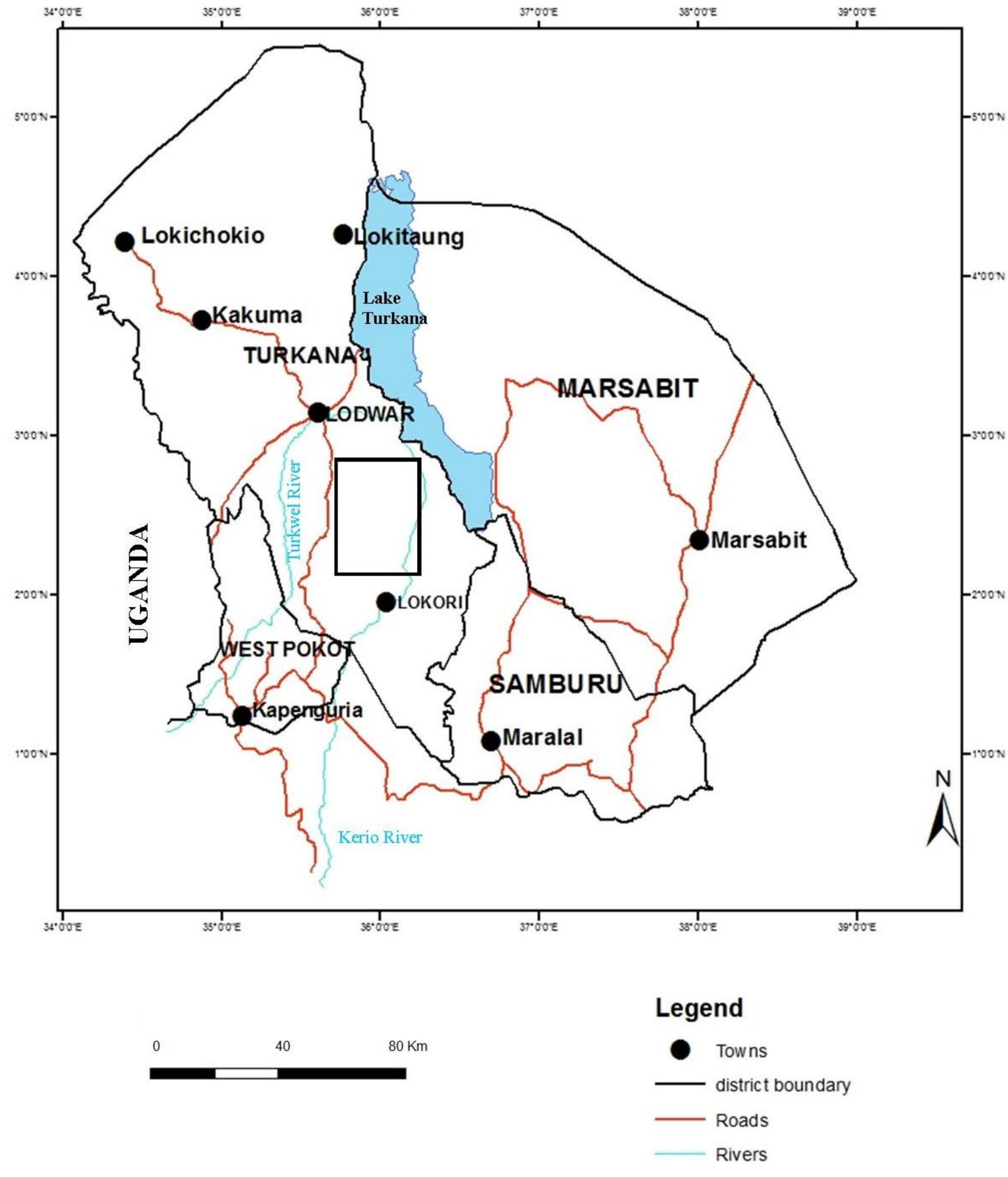

Figure 1-1: Map of north western Kenya with the rectangular box showing location of the study area (modified from NOCK 1987).

1.2.2. Climate

Lokichar basin is within an arid region with temperatures ranging between 24°C to 38°C and a mean of 30°C. There are two rainfall seasons. The long rains which normally occur between March and July and the short rains which occur between October and November. Rainfall ranges between 120 mm and 500 mm per year; the western parts and areas of higher elevation in the basin receive more rainfall. Rainfall occurs under the influence of the south-east monsoon, which originates over the Indian Ocean and is relatively cool and moist. However, distribution of rain in the area is controlled by the land masses (Olang 1979). The rainfall is erratic in distribution and timing. The dryer the area, the more unreliable the rain is.

1.2.3. Vegetation

Vegetation in the entire Lokichar basin consists of mainly scattered *Acacia* bushes and a cover of annual herbaceous plants. The density of the woody plants increases on hilly ground. This vegetation pattern is repeated again and again until it becomes monotonous. The control of vegetation pattern is geological (Joubert 1966). However, it is punctuated by *Maerua* species and *Acacia tortilis* along the river-banks (Olang 1979). On the western side of these uplands and peneplains are the piedmont plains, which have been developed under dry climatic conditions (Olang 1979). Most of the vegetation is classified as short shrubs.

1.2.4. Physiography and Drainage

Lokichar basin can be divided into four regions in each of which the type of relief and vegetation are more or less uniform according to Joubert (1966):

- The hills composed of basement rocks and the inselbergs on the plains.
- The featureless plains for the main part covered by alluvium.
- The hills composed of volcanic rocks.
- The area sloping to the east away from the hills composed of volcanics.

Volcanic events are responsible for local modification of the drainage; radial or approximately radial drainage patterns developed, for instance, at the main volcanic centers (Rhemtulla 1970).

The Turkwell River and Kerio River are the main streams flowing through the basin and all their tributaries are sand rivers that carry water only immediately after heavy rainfall. Lokichar River and Kalabata River crosses through the study area. The most important single factor governing the drainage pattern in South Turkana region is the overall slope of the rift floor which falls steadily from some 1830 m at Nakuru to about 366 m at Lake Turkana.

Dendritic drainage patterns are most common but other types of drainage patterns are also found such as parallel drainage patterns on alluvial plains (Joubert 1966). The courses of the main rivers are closely controlled by the northward slope topography (Rhemtulla 1970). The Kerio is a semi-permanent river which dries out only during the season of least rainfall (generally August-November). Drainage map of south-western Lake Turkana area is shown in Figure 1-2.

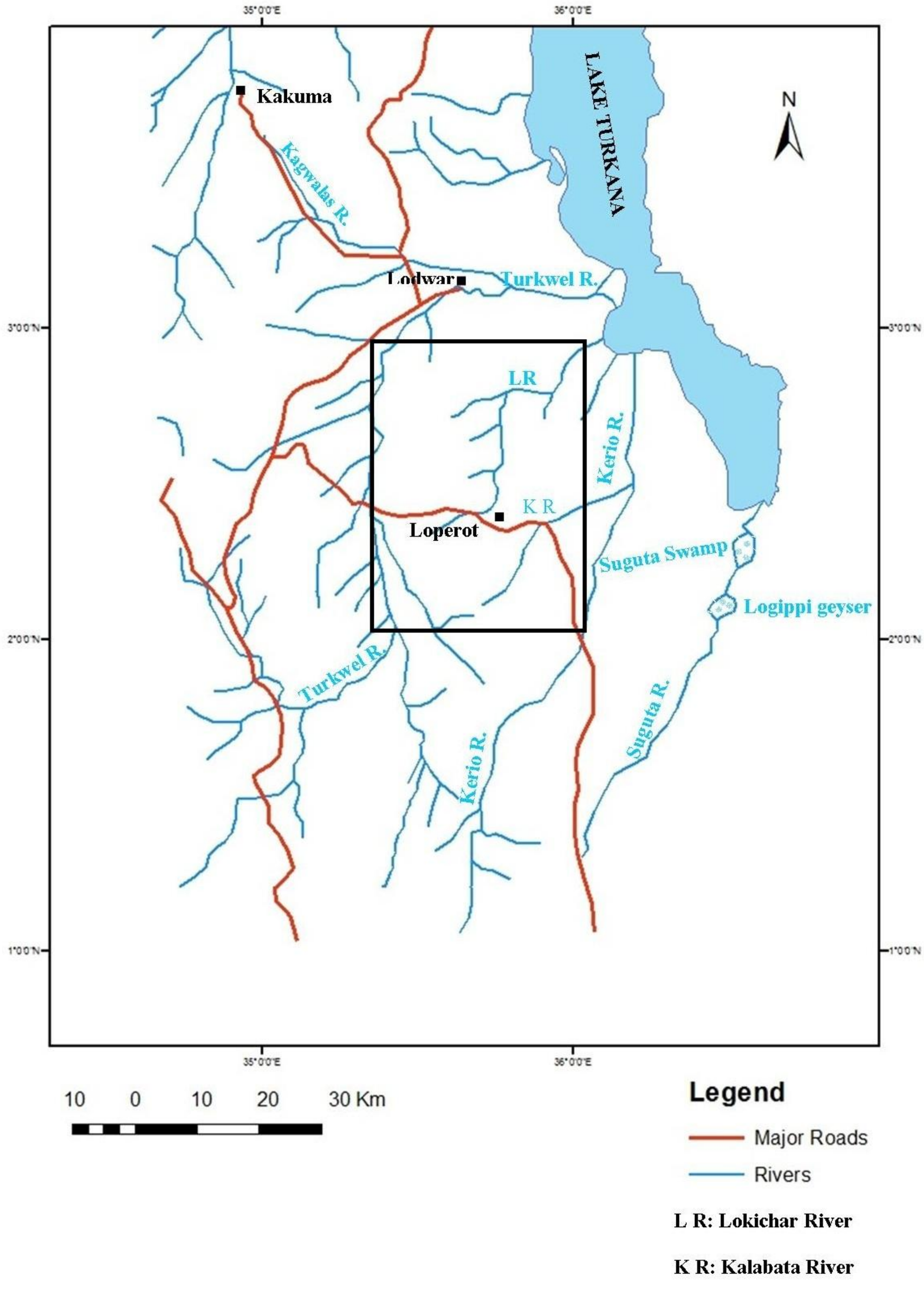

Figure 1-2: Drainage map of south-western Turkana region with the rectangle showing the study area (modified from Arthur, 1937).

1.3. Justification and Significance of the research

The Tertiary rift system has a similar structural system as that of the Albertine Graben. In the Albertine Graben, there was a major discovery of oil in 2006. Therefore, the northern part of the Tertiary rift in Kenya has very similar geological and structural features to that of Albertine Graben. In addition, there also was some Tertiary sourced oil recovered in Loperot-1 well drilled by Shell in 1992 in Lokichar basin. At the time of doing this research, oil was discovered in Lokichar basin in Ngamia-1 well drilled by Tullow Oil PLC in March 2012. Through this research, interpretation of seismic data will provide relevant structural and geological information to other researchers. This research information will also aid in oil and gas exploration in the country. Oil and gas discovery will be of great importance to the local economy.

1.4. Literature Review

In 1970, an extensive seismic survey by Project PROBE (Proto-Ocean and Basin Evolution) acquired seismic reflection data over Lake Turkana (Dunkelman et al., 1989) and the surrounding region. The survey revealed the presence of significant structures beneath the lake. The region was determined to have a series of half grabens which alternate in polarity along the axis of the lake and were linked end to end by zones of structural high.

Khan and Swain (1978) carried out geophysical investigations in the Rift Valley system of Kenya and estimated the thickness of sediments and volcanics of the region. Their research showed that the deep structure of the rift is anomalous and similar to that of the Mid-Ocean ridges, with most of the information coming from seismic studies.

(Shackleton 1978) described the structural development of the East African Rift system which also covers the study area. He recognized the general structural sequences like the major bounding faults and closely spaced faults across the whole width of the rift floor.

In 1985, Amoco Kenya Petroleum Company acquired detailed gravity surveys which provided the first clear indications of half graben in southwestern Turkana and also defined the northwestern extent of the Anza Graben (Morley et al., 1992). Amoco Kenya Petroleum Company also acquired 1,407 km of 2D seismic data in the area, including offshore Lake Turkana ("Turkana energy," 2008). This data was augmented with gravity and field geology surveys. It was determined that faulting, subsidence and inversion of the half grabens resulted in a range of structural traps. Most of the traps are faulted dip-closures located at the graben margins or at transfer zones within the grabens.

Frostick & Reid (1987) reassessed the universality of classical graben model and its implications for patterns of sedimentation, with the availability of seismic data. His closer examination revealed that the faults are not only curved frequently, but also the rift is composed of segments and in any one single segment, one boundary fault is dominant.

(Grove 1986) used geophysical work and geological mapping data to describe the morphology of the rift system where it was concluded that rift faulting in the Miocene was accompanied by outpouring of great volumes of lava in the areas. Low angle volcanic piles were built at the margin of the rift and within it in late Miocene and Pliocene.

Morley et al (1992) described the tectonic evolution of the northern Kenya rift based on geological fieldwork, radiometric dating of volcanic rocks, gravity and seismic survey. Research results revealed deep half graben basins up to 7 km thick which were initiated west of Lake Turkana probably during the late Oligocene-Early Miocene times. It also revealed that Lokichar basin is bounded by easterly dipping fault trending along the western side of the rift from Lake Turkana.

Between 1992-1993, Shell Exploration and Production Kenya B.V. (SEPK) acquired exploration acreage to test the un-drilled Tertiary fluvio-lacustrine sediments of the East African Tertiary Rift System (Lambers 1993). SEPK acquired 1080 km of 2D seismic coverage. SEPK also reprocessed and interpreted the seismic data that had been acquired by Amoco and drilled two wells in the northwestern Kenya region i.e. Eliye Springs-1 which was water bearing and Loperot-1 which recovered some oil and penetrated two intervals of lacustrine sediments containing good to excellent source rocks ("Turkana energy," 2008).

(Mariita 2003) used KRISP results and well data as constraints in analyzing the gravity anomalies associated with the Kenya dome and northern Kenya to obtain a detailed, integrated interpretation of the upper crustal structure. Features of interest in the analysis included the graben symmetry and the relationship of the gravity maxima along the rift axis to magmatic centers.

Vitel et al (2004) worked in the entire East African rift and presented a complementary approach that attempted to correlate the basin structures imaged on seismic profiles with morphotectonic features and river drainage data supplied by satellite imagery. Correlation of seismically imaged rift structures with river drainage anomaly at the surface permitted a determination of the structural evolution of the flexural margin of the Lokichar basin from Paleogene–Miocene up to present.

Rop (2011a) reviewed the subsurface stratigraphy in the northwestern Kenya Rift basins with the help of geophysical and geochemical data. Gravity anomaly maps and seismic profiles were used and revealed the presence of several horsts and grabens structural systems. It was also revealed that the basins in Turkana region attracted potential petroliferous sedimentary piles (~2000–5000 m thick) which were deposited on basement rocks of Precambrian age and later overlain by basaltic flows of mainly Miocene age.

1.5. Aim and Objectives

1.5.1. Aim:

The aim of this study was to determine the sub-surface structures, identify and delineate possible hydrocarbon prospective areas within Lokichar basin through seismic interpretation.

1.5.2. Objectives:

1. To determine the sequence of rock types and basement highs in the basin through interpretation of the seismic sections using well log data.
2. To determine the structures that occurs within the basin and their characteristics.
3. From objectives (1) and (2) above, determine the occurrence of possible hydrocarbon traps and possible hydrocarbon prospective areas.

CHAPTER TWO

2.0. GEOLOGICAL SETTING

2.1. Regional geology

Generally in the entire northwestern Kenya region, crystalline gneisses, schists and granulites of the Basement system rocks form the base on which all the sediments and lavas were deposited and extruded. After deposition and deformation of the basement system, there was a very long period in which there is no record preserved and it is only since lower Miocene times that the geological sequence of events can again be deciphered (Joubert 1966). Detailed geology of the Lake Turkana region is described by (Fuchs 1939) and (Vitel et al., 2004). Lithostratigraphy of Turkana Depression is shown in Figure 2-1.

Geological Age of unit	Numerical Boundary Age (Ma)	Stratigraphic unit or locality in Turkana Basin
Holocene		Galana Boi Fm.; Kibish Fm., Member IV
	0.012	
Late Pleistocene		Kibish Fm., Member III
	0.13	
Middle Pleistocene		Kibish Fm., Members I, & II, Koobi Fora Fm. (Chari Member , in part), Nachukui Fm. (Nariokotome Member, in part); Barrier Volcanics (in part)
	0.78	
Early Pleistocene		Koobi Fora Fm. (upper Burgi to Chari Mbs.); Shungura Fm. (Members D-L); Nachukui Fm. (Lokalalei to Nariokotome Mbs.), Fejej; Barrier Volcanics (in part); Mt. Kulal; Asie; Huri Hills
	2.6	
Pliocene		Koobi Fora Fm. (Lonyumun to lower Burgi Mbs.); Usno Fm.; Mursi Fm., Shungura Fm. (Members Basal-C); Kanapoi Fm., Warata Fm. , Fejej Nachukui Fm. (Lonyumun & Tulu Bor Mbs. & Apak Mb. at Lothagam), Gombe Group Basalts
	5.3	
Late Miocene (Tortonian & Messinian)		Nawata Fm. (Lothagam)
	11.6	
Middle Miocene (Serravallian & Langhian)		Lothidok Fm. (in part); Abwaria Alangan beds (Lothagam); Napedet; Sibilot; Gum Dura Fm.; Il Yia Fm.; Nakwele Fm.
	16.0	
Early Miocene (Aquitanian & Burdigalian)		Lothidok Fm. (Kalodirr, Moruarot); Bakate Fm. (Buluk); Loperot; Locherangan; lavas of Lothidok
	23.0	
Oligocene		Eragaleit beds; Nakwai; Benson's site; lavas of Kachoda, Kaling; Langaria Fm.; Muruang'apoi Hills; Pelekech; Lorienetom
	33.8	
Eocene		Lokitaung volcanic rocks; Nabwal Fm.
	55.8	
	66.5	
Late Cretaceous		Lubur Sandstone, ?Muruanachok sandstone, ?Sera Iltomia sediments
	99	
	>522	
Metamorphic basement		Metamorphic rocks of Labur, Muruanachok, Lokhone, Uganda Escarpment, Muruanasigar, Nyiru, Hamar Range, Nkalabong, Mwi-Maji

Figure 2-1: Lithostratigraphic units in the Turkana Depression arranged by age except for the Pliocene-Pleistocene (Vitel et al., 2004).

2.2. Geology of the Lokichar Basin

Geology of entire Turkana rift region including the study area is shown in Figure 2-2. The study area consists of the following rock units: Basement rocks, Loperot grits, Lokhone sandstone formation, Auwerwer sandstone formation, Lothidok formation, Auwerwer basalts and Pliocene-Recent sediments.

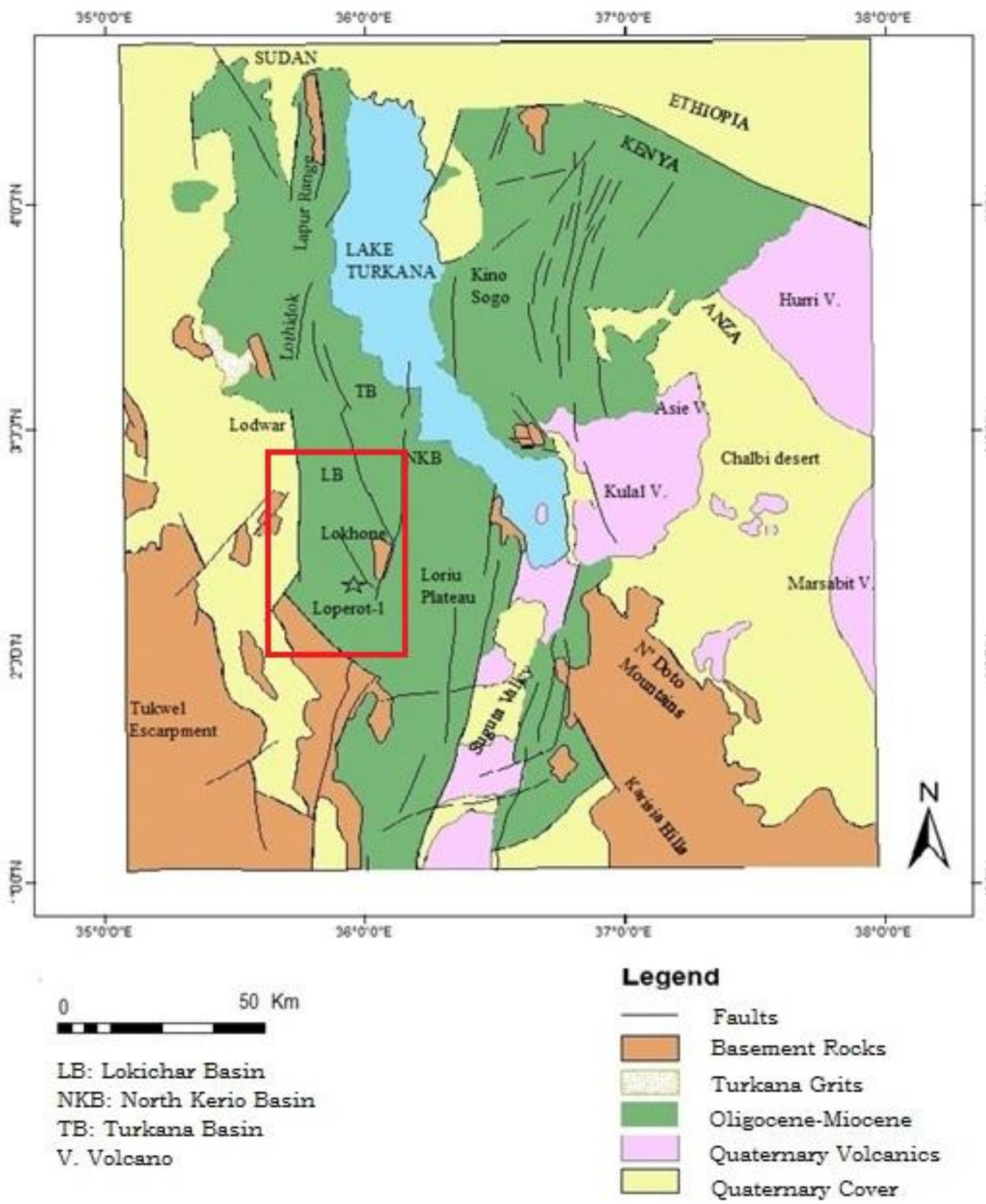

Figure 2-2: Geology of Turkana rift with the rectangle indicating the study area (modified from Le Gall et al., 2005).

2.2.1. Basement rocks

Basement System rocks are strongly deformed gneisses and schists of amphibolites facies and occur in fault bounded blocks. They are exposed in Lokhone area east of the basin. They include biotite-gneisses with calc-silicate granulite near the base, biotite-hornblende gneisses and hornblende-pyroxene gneisses. These basement rocks are the dominant sediment sources for much of the clastic sequences deposited during the Neogene (Feibel 2011).

2.2.2. Loperot grits

Mostly occur at Loperot area towards the east of Lokichar basin. The oldest exposed section comprising thin limestones with gastropods or bone-bearing grits directly overlies Precambrian basement at the southern and western edge of the Lokhone horst (Morley et al., 1992). They lie with a marked unconformity on the basement rocks. Loperot grits were originally referred to as Turkana grits by Joubert (1966). They include buff-coloured arkosic, channelized fluvial pebbly sandstones and minor conglomerates grits. These rocks exhibit a wide scatter of palaeocurrent directions to the west, north and east suggesting a generally northerly directed flow (Morley et al., 1992). A number of doleritic dykes are emplaced in these sediments. The dykes tend to erode more readily than the country rock to form linear trenches (Rhemtulla 1970).

2.2.3. Lokhone sandstone formation

The Lokhone sandstone formation includes two major lacustrine shale intervals (the Lokhone Shale Member, and the Loperot Shale Member) which are both several hundreds of meters thick as encountered in the Loperot-1 well (Figure 2-3) but may be as thick as 1.3 km to the west, when approaching the Lokichar boundary fault (Thuo 2009). Exposures of the Lokhone sandstone formation are poor, excepted to the north-north-east of Loperot, in the Lakhapelinyang area (Tiercelin et al., 2004). Palynological data from the Loperot-1 well indicate a Paleogene to middle Miocene age for the whole formation.

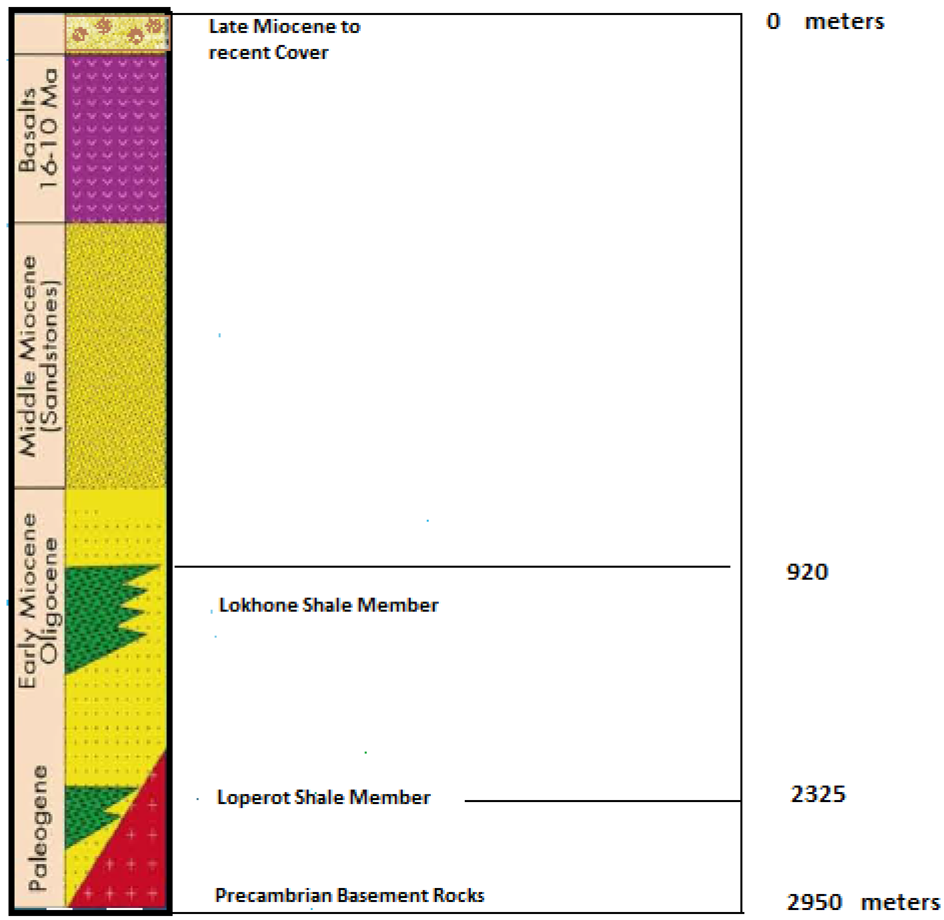

Figure 2-3: Stratigraphy of Lokichar basin based on the results of Loperot-1 well (modified from Tiercelin et al., 2009).

2.2.4. Auwerwer sandstone formation

Rock units in this formation occur above the Lokhone sandstone formation and present a sequence of coarse-grained to fine-grained sediments which are distinct from the arkosic grits by their colour (tan, white, brown, red, yellow and purple) and composition, which contains a significant volcanic component, particularly tuffaceous material. Their depositional environment was dominated by fluvial and ephemeral lacustrine conditions. The absence of interbedded lavas and large volcanic boulders within the grits suggest that the main volcanic centers were situated outside the half graben at this time (Morley et al., 1992).

2.2.5. Lothidok formation

Rock units in this formation are found in the northern part of Lokichar basin. The formation comprises of a series of volcaniclastic sandstones, arkosic sandstones, lava flows altered mafic tuffs and trachytic tuffs and pyroclastics that overly Oligocene or Miocene basalts that are themselves overlain by Miocene-Pleistocene volcanics and sediments (Thuo 2009). The formation reaches a total thickness of 580 m. The name Lothidok is derived from the Lothidok range located between Lodwar and Kalakol where typical section of the formation outcrops. Rocks belonging to this formation were previously referred to as Turkana grits by (Fuchs 1939).

2.2.6. Auwerwer basalts

These basalts almost cap the entire Lokichar basin except in the north where Kalakol basalts occur. These basalts date from 12.5-10.7 Ma (Morley et al., 1992; Thuo, 2009). Auwerwer basalts are about 300 m in thickness and contain thin interbedded sediments. The lavas are covered by recent sand and gravel.

2.2.7. Pliocene-Recent sediments

Recent rock sediments include alluvium deposits, recent basalts and ashes. Subsidence of the Turkana rift has initiated accumulation of these sediments along the existing drainage networks in the region (Feibel 2011). Recent sediments overlie volcanic rocks. They consist of poorly-sorted, coarse (up to boulder size) matrix supported volcano-clastic sandstones and conglomerates, with large-scale erosional surfaces hundreds of meters wide. These beds were interpreted as proximal alluvial fan deposits by Morley et al (1992).

2.3. Structural geology of Lokichar Basin

Structurally, Lokichar basin lies entirely within the N-S trending East African Tertiary Rift System. This being a continental African rift, it is dominated by half grabens (Frostick & Reid 1987). The syn-rift sedimentary sections of all basins in Turkana area show a great number of fold/fault structures that resemble inverted features (Le Gall et al., 2005). Turkana Rift is composed of short, linear, NNE-trending normal fault segments (Figure 2-4) that are offset in a left-lateral sense by numerous, NW-SE trending transfer faults, linking facing border fault segments together (Vitel et al., 2004; Dunkelman et al., 1989). The overall trend of the rift zone is oblique to the opening direction (Le Gall et al., 2005).

Fault geometries are highly variable in Lokichar basin, but flower structures associated with transfer faults predominate (Dunkelman et al., 1989). Igneous activity is ubiquitous and appears to be localized along the transfer faults. Lokichar basin fill reaches 4 to 5 km in thickness and is dominated by fluvial clastic, volcaniclastic and volcanic materials (Dunkelman et al., 1989).

The basin consists of relatively simple structural geometry with a major basin-bounding fault on the western margin called Lokichar fault as illustrated in Figures 2-4 and 2-5. The basin also consists of a flexural margin on the eastern margin. Lokichar fault cross-cuts at an acute angle on the foliations in Precambrian basement (Figure 2-5). The fault is curved in map view, but is low-angle and planar in cross-section, and dips some 30-40^{o} lower than the surface foliations (Morley 1995).

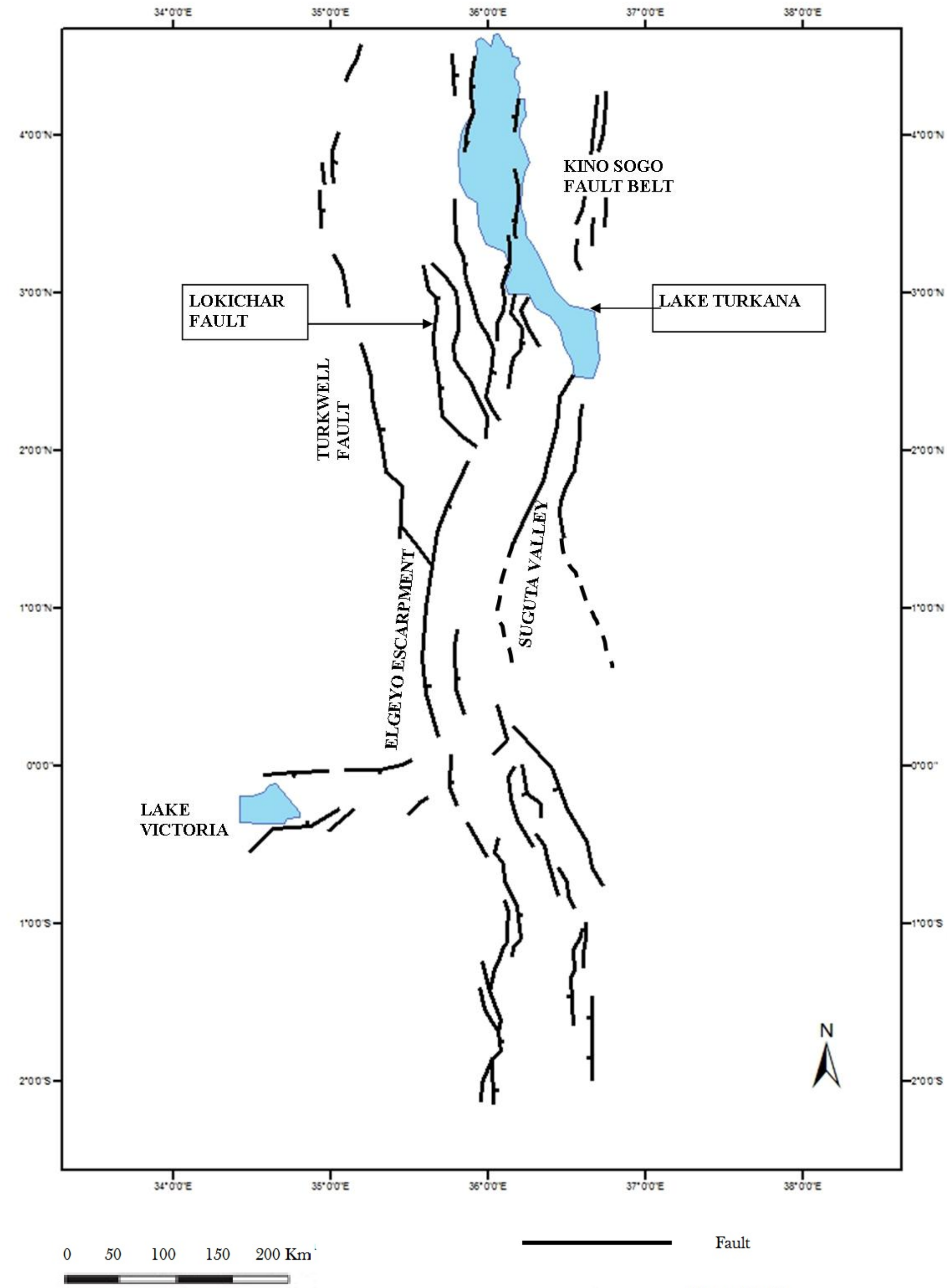

Figure 2-4: Structural framework of the N-S trending Tertiary rift showing Lokichar fault (modified from Keqiang 2007).

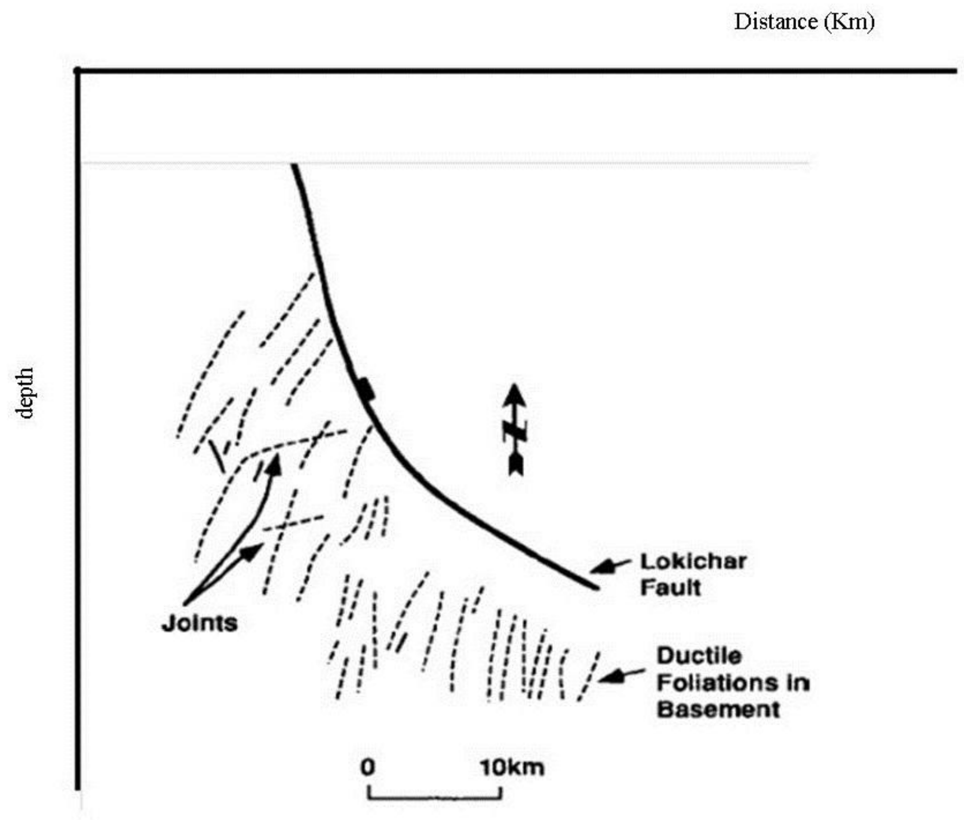

Figure 2-5: Cross-cutting of pre-existing foliations in crystalline basement rocks (modified from Morley 1995).

CHAPTER THREE

3.0. SEISMIC REFLECTION METHOD

3.1. Theory of seismic reflection

Seismic data is produced by sending artificial energy into the earth and recording its response. In the early days waves were generated by blasting in shallow wells but today vibrations with different range of frequencies for wave generation are usually used (Bartucz 2009). Seismic energy travels into the ground in a spherical wave front, similar to dropping a pebble into a pond.

Reflection coefficients are a function of the acoustic impedance. Acoustic impedance can relate directly to rock type, pore space, pore fluid, and reservoir quality. The reflection coefficient is dependent upon the contrast of acoustic impedance between two layers.

$$R_c = \frac{Z_2 - Z_1}{Z_2 + Z_1}$$

where R_C is the reflection coefficient; Z_2 is the acoustic impedance of layer 2 and Z_1 is the acoustic impedance of layer 1. For large acoustic contrasts the stronger the reflection coefficients are in the subsurface the larger the reflection will be recorded at the surface (Hager 2009).

Reflected energy is recorded as traces on a seismic section. A seismic section for a shallow reflector looks like as shown in Figure 3-1 while for a deeper reflector, the trace lines are put close to each other together and appear as shown in Figure 3-2. The traces are found on the x axis. One trace represents one geophone location. TWT is on the y axis. It is the corrected time that is needed for the seismic wave to return from a specific depth if the wave source would have been in the place of the geophone. In visualization the trace lines are put close to each other.

Theory of seismic method is described in detail by many textbooks e.g. (Kearey et al., 2002; Mondol, 2010; Scintrex, 1996 and Telford et al., 1990).

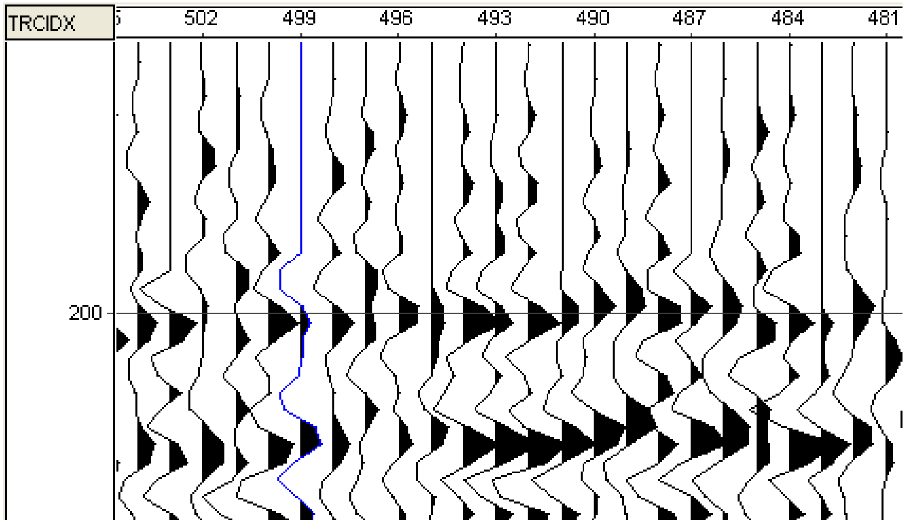

Figure 3-1: Seismic section due to a shallow reflector (Bartucz 2009).

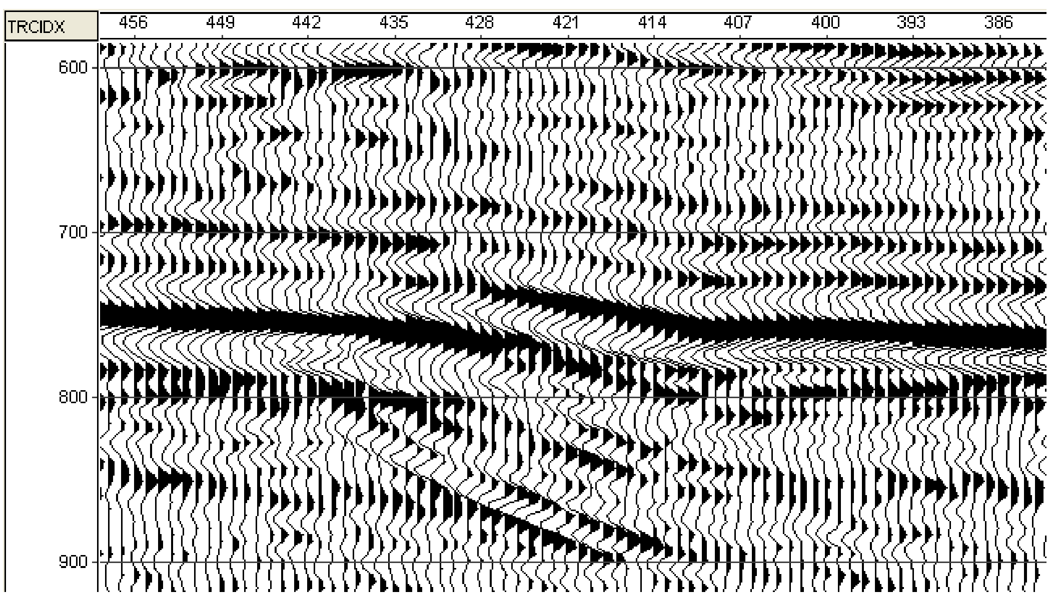

Figure 3-2: Seismic section from due to a deep reflector (Bartucz 2009).

3.2. Two dimensional seismic reflection survey

In reflection profiling (2D surveying) all source points and receivers are aligned along preferably straight lines. Only when profiles run perpendicular to the prominent geologic strike, the reflected raypaths can be assumed to travel in the profile plane (Schuck and Lange 2007). During this survey the source point and its associated geophone spread are progressively moved forward along the profile line to achieve lateral (multi-) coverage of the underlying geological section. Figure 3-3 shows the various source-geophone arrangements used in 2D seismic reflection survey.

a) split spread (split dip): the geophone array is arranged symmetrically on both sides of the source
b) end-on direct: the geophones are arranged in-line at one side of the source and in the direction of the source movement.
c) end-on inverse: the geophones are arranged in-line at one side of the source but in the opposite direction of the source movement

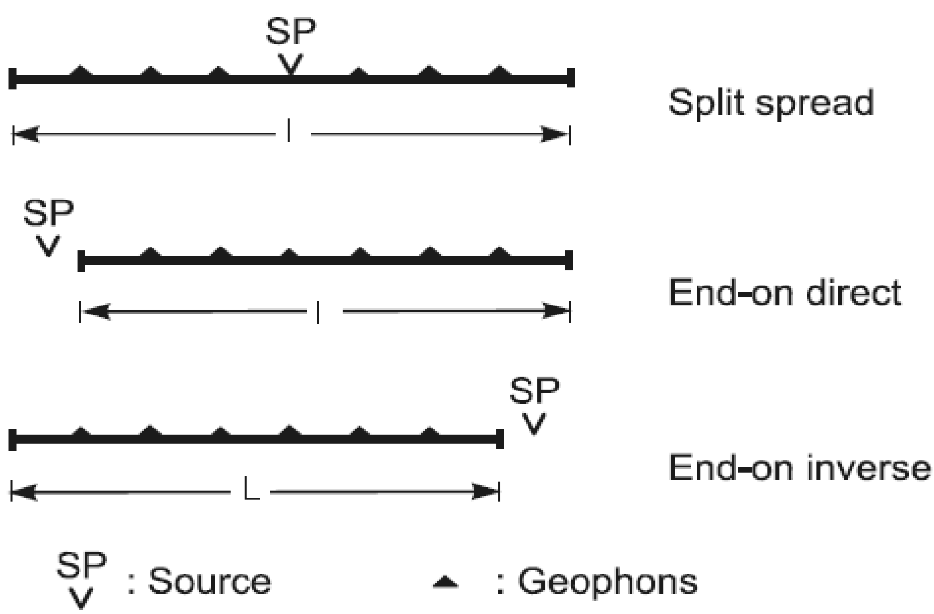

Figure 3-3: Commonly used source-geophone arrangements (spreads) for 2D seismic reflection data acquisition (Schuck and Lange 2007).

3.3. Seismic reflection data processing

The main purpose of this research was to carry out interpretation of processed and migrated 2D seismic data. However, this cannot be done without mentioning processing techniques that are commonly applied to 2D seismic data before interpretation. Seismic data processing aims at production of interpretable data volumes by noise attenuation and data migration (Admasu 2008).

The following are some of the processing techniques that are applied to 2D seismic data (Figure 3-4):

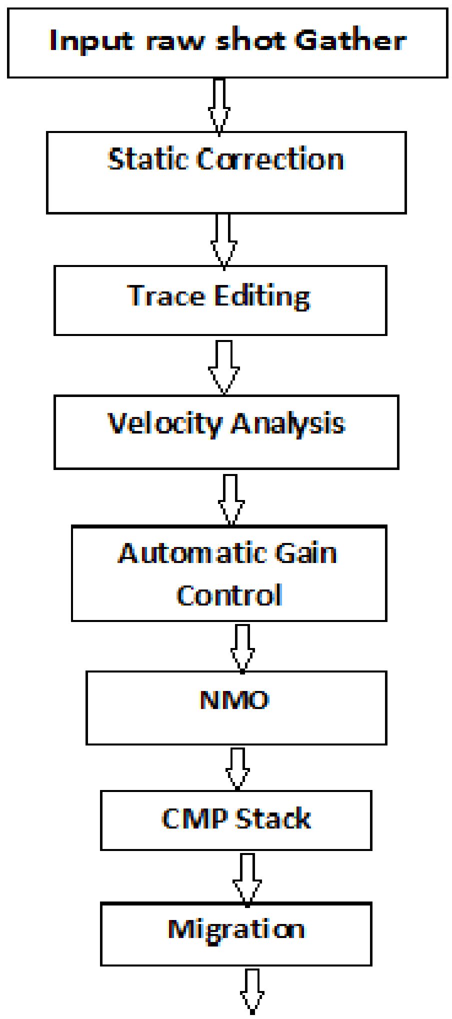

Figure 3-4: Seismic data processing flow chart.

3.3.1. Static correction

Static corrections are applied to seismic data to compensate for the effects of variations in elevation, weathering thickness, weathering velocity, or reference to a datum (Schuster 2010). The objective is to determine the reflection arrival times which would have been observed if all measurements had been made on a flat plane with no weathering or low velocity material present. These time shifts distort the true geometry of deep reflectors.

3.3.2. Trace editing

Trace editing is needed for terminating the traces that have minimal anomalous noise. This is done after defining the geometry of the dataset (Nilanjan 2008). Incoherent random noise present in the datasets is removed by this process. The sources of such types of noise could be a dead or poorly installed geophone, wind motion or any movement near the recording cable (Nilanjan 2008).

3.3.3. Velocity analysis

Velocity analysis is done to get the velocity distribution as a function of time which will give the most accurate NMO correction. The major objective of velocity analysis is to ascertain the amount of normal moveout that should be removed to maximize the stacking of events that are considered to be primaries (Telford et al., 1990). Velocity analysis is used to compute corrections in traveltime that will be applied to all the traces belonging to a CMP-gather.

The most common type of velocity analysis is to repeat the procedure of correcting and stacking CMP data for many different velocities and within a discrete time window (Mondol 2010). By measuring the average absolute value of the data or more precisely the semblance within time windows of different test velocities, and plotting these results in a time versus velocity histogram.

3.3.4. Automatic gain control

Automatic gain control (AGC) is applied to seismic data to adjust amplitude decay with time. The amplitude of any trace is affected by various factors including the shot strength, response and coupling of the receivers, trace offsets and geological condition (Fugro 2007). AGC estimates the amplitude variations due to various components and computes weighting levels for each component, using the Gauss-Seidel iterative method (Fugro 2007). The gain function operates on a point in the specified time gate which then slides down one sample at a time with corresponding gain corrections. The process continues until the whole trace has been adjusted.

3.3.5. Normal move-out correction

NMO is the difference between the two-way travel time at a given offset and the two-way zero-offset time (Mondol 2010). The NMO correction stretches the waveform in a trace and produces a new waveform with a greater period (Figure 3-5) so that after the correction shallow events are shifted to lower frequencies in the gather (Nilanjan 2008). The objective is to determine stacking velocities (rms-velocities) which will result in the highest signal to noise ratio of the final stacked seismic section used for the geological interpretation (Schuck and Lange 2007).

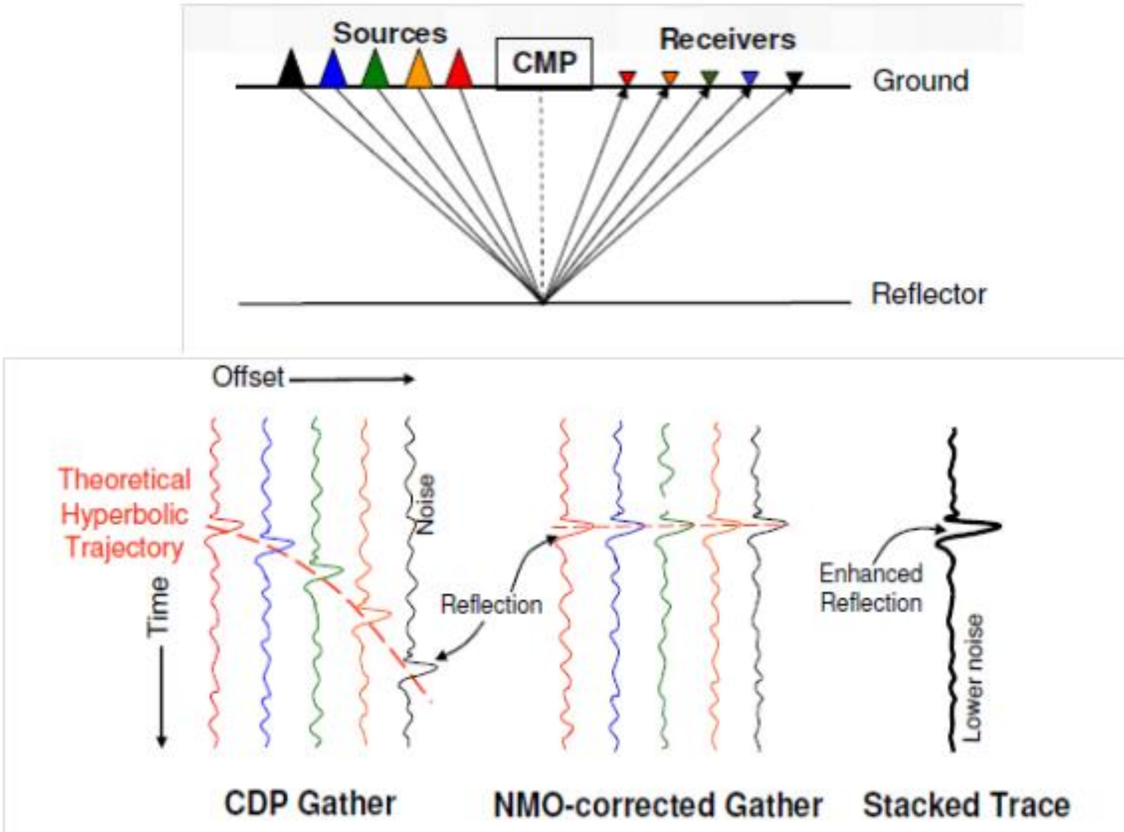

Figure 3-5: Common midpoint stacking during seismic data processing (SMT 2012).

3.3.6. CMP Stack

Common Midpoint Stacking is summing the traces in the CDP gather along the offset axis as shown in Figure 3-5. This technique is used to improve the signal-to-noise ratio and to attenuate multiples (Schuck and Lange 2007). The NMO corrected CMP trace gathers are stacked using this process which is an important step in seismic processing. The collection of stacked traces forms a seismic section which gives an image (slice) of the subsurface (Mondol 2010).

3.3.7. Depth migration

Migration will lead to the final product, either as depth or time. Depth migration will adjust events in seismic trace to compensate for dipping reflectors (Figure 3-6). Migration can be done using velocities based on the results of velocity analysis if they are good enough. This is applied by testing a range of different velocities to determine which collapse diffractions correctly, or by using other information.

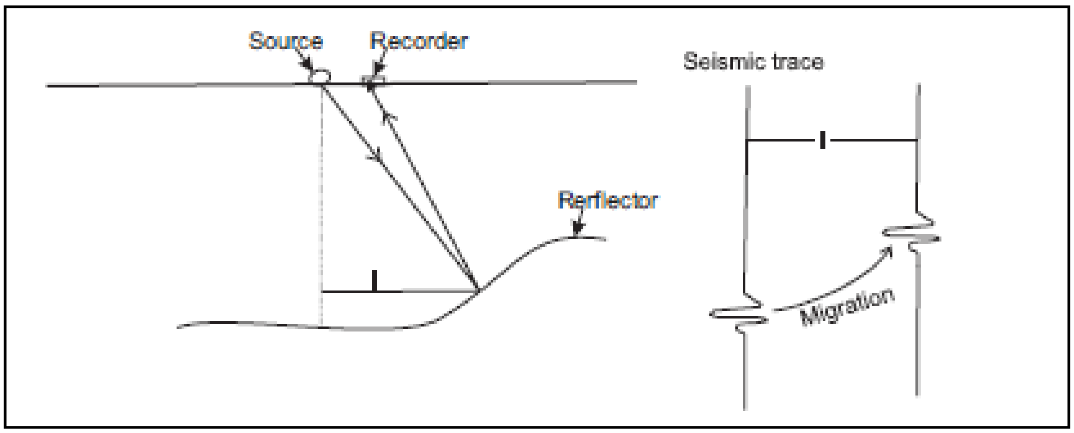

Figure 3-6: Illustration of the concept of migration (Admasu 2008).

3.4. Concept of seismic reflection data interpretation

Seismic data is interpreted to provide information about composition, fluid content, extent and geometry of rocks in the subsurface. The seismic sections or images represent slices through the geological model, which can be input to advanced workstations where the actual interpretation can take place (Mondol 2010). Seismic data can be used in many ways such as regional mapping, prospect mapping, reservoir delineation, seismic modeling, direct hydrocarbon detection and the monitoring of productive reservoirs.

In terms of the parameters that are analyzed and the interpretation that may be drawn from such analysis, a hierarchy of seismic interpretations can be achieved. These interpretations include seismic facies analysis, seismic structural analysis, seismic attribute analysis and seismic sequence analysis. The most important parameters used for interpretation of seismic data are defined by Mondol (2010) and are listed below:

a) Reflection amplitude: This is the strength of the reflections. It is represented by the proportion of the energy reflected at the boundary between two beds and is a function of the difference in the acoustic impedances. In case of alternating series of different beds, the distance between the bed boundaries in relation to the wavelength of the transmitted seismic signals will play a major part.
b) Reflector spacing: The distance between the reflectors will indicate the thickness of the bed, but there will be a lower limit to the thickness that can be detected, which will depend on the wavelength.
c) Interval velocity: The interval velocity of a sequence can provide information about lithology and porosity but this will depend on the stacking velocity and will not be very accurate.
d) Reflector continuity: The continuity of reflectors will be a function of how continuous the sediment beds are, information which is essential for reconstructing the environment.
e) Reflector configuration: The shape of the reflecting beds gives a picture of the sedimentation surface as it was during deposition. The slope of the reflectors, for example, represents the slope of prograding beds in a delta sequence with later differential compaction and tilting superimposed. Erosion boundaries with unconformities will in the same way show the palaeo-topography during erosion.
f) Instantaneous phase: A seismic trace can be considered as an analytical signal where the real part is the recorded seismic signal itself. The complex seismic trace (imaginary parts of the signal) and the instantaneous attributes are computed mathematically. The Instantaneous phase is a measure of the continuity of the events on a seismic section. The Instantaneous phase is on a scale of $+180^o$ to 180^o. The temporal rate of change of the instantaneous phase is the instantaneous frequency.

CHAPTER FOUR

4.0. METHODOLOGY

4.1. The data set used

Data used to carry out this research was secondary 2D seismic data that was provided by NOCK. This data set was acquired by Amoco Kenya Company in 1985 in Turkana area where a total of 1,407 line Kilometers of 2D seismic data was acquired.

During the acquisition of the 2D seismic data, Vibrator trucks were used in-line as the seismic sources (Vibroseis TR4/X2). The vibrators used linear 1–second upsweep of between 6–64 Hz, with 6 seconds of additional listening time for 7 seconds uncorrelated record lengths. A 124-channel recording system with 48 geophones per station along a linear array was employed. The geophone-frequency was 10 Hz and data was recorded at 4 micro seconds sampling rate. Processing of these seismic lines was originally done by Amoco Kenya Company but later reprocessing was done by SEPK.

4.2. The software used

Arc-GIS 10.0 was used to digitize the 5 seismic lines on the location map and determine the location of the shots point for each line. This software was also used to digitize, modify and reconstruct geological, structural and drainage maps from Lokichar basin and surrounding regions.

SMT Kingdom Suite vers 8.6 was used to carry out the analysis and interpretation of the 2D seismic data. Within the SMT Kingdom Suite software is a program known as 2D/3DPAK window. The 2D/3DPAK window allowed visualization of the vertical seismic display of all the seismic lines. The software also allowed picking horizons and faults of interest in time.

4.3. General description of seismic sections

As stated earlier, five lines of 2D seismic data were used to carry-out the research. They include seismic lines TVK-13, TVK-107, TVK-108, TVK-127 and TVK-129. These seismic lines were chosen based on the availability of digital data because not all the lines from the region contained data in a digital format at the time of receiving the seismic dataset. However, the chosen lines are a good representative of the basin. Seismic lines TVK-107, TVK- 108 and TVK-127 are oriented in SSW-ENE direction relative to Lokichar basin while seismic line TVK-13 is oriented WNW-ESE and seismic line TVK-129 is oriented NW-SE relative to the basin (Figure 4-1).

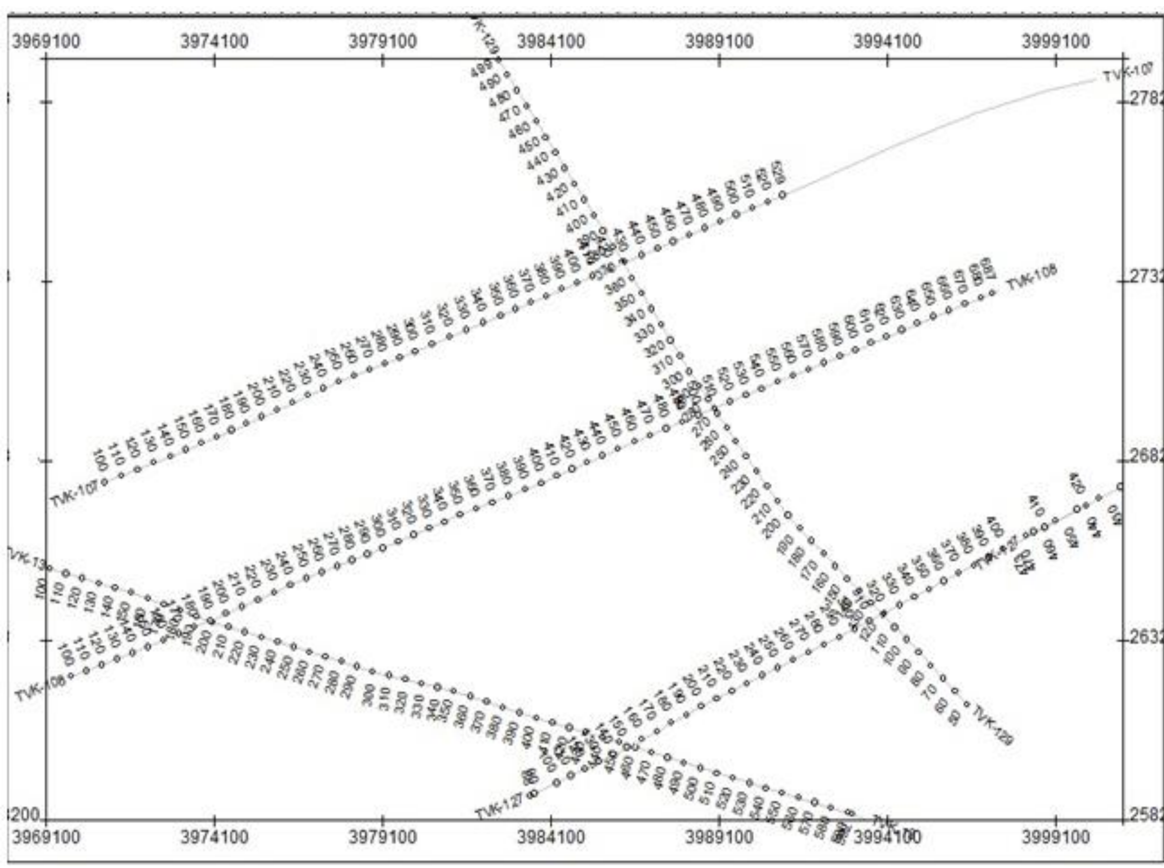

Figure 4-1: Orientation of the seismic lines on the Kingdom Suite base map; the small circles on the lines indicate shot point locations.

4.4. Interpretation of the seismic data

4.4.1. Interpretation process

The following is the procedure that was followed during interpretation:

- Digitization of shots point locations for each seismic line, writing down the shots point locations and saving them as a text file for importation into Kingdom Suite software. Shots point locations for all the seismic lines are given in Appendix A.
- Importing the files containing shots point locations into Kingdom Suite software in the same base map. This gives the orientation of the seismic lines as shown in Figure 4-1 on the base.
- Viewing of the seismic data using Kingdom Suite Viewer. This allowed header information from the seismic lines to be determined.
- Importing seismic data in SEGY format for the 5 seismic lines into Kingdom Suite software. A unique interpretation window was assigned to each seismic line in order to interpret each line separately.
- Digitization of location and study area map, drainage map and geological map of the basin.

4.4.2. Horizon interpretation

Horizon interpretation was done by trying to identify the major stratigraphic packages, unconformities, flooding surfaces or sequence boundaries which were observable on the vertical seismic display of a seismic line. The procedure was to first identify observable horizons or group of horizons with similar attributes. This was followed by creating the horizons or group of horizon and lastly picking of the horizons of interest to digitize them. Peaks in the seismic data that correspond to these surfaces were traced along the available seismic transects and the interpretations were viewed independently of the data.

In this research, there was an intension of using auto-picking (2D hunt) technique during horizon interpretation and manual pick where there were discontinuities. However, this was not possible since most of the horizons were mostly discontinuous on all the seismic lines. The data set had also poor resolution. Therefore only manual picking method was employed.

4.4.3. Fault interpretation

On 2D seismic sections, faults appear as diffuse zones of discontinuous horizon reflectors. Abrupt vertical displacement of several reflectors along a distinct line (faults plane) is the best indicator for the presence of faults (Marillier et al., 2006). Fault interpretation was done in the same way as horizon interpretation by identifying and defining the major fault patterns observable on the seismic sections e.g. Lokichar fault.

Fault interpretation on a single vertical seismic display for a given seismic line was defined by creating the fault and digitizing a series of points which comprised a fault segment. Only the major fault which was observable was assigned a name Lokichar fault, while other minor faults were interpreted as unassigned faults. Results of this procedure are discussed in Chapter 5.

4.4.4 Interpretation method

Only seismic data was interpreted since no digital well log data from Lokichar basin was available at the time of getting the data set. Interpretation of these seismic lines has been done previously by oil companies but their results were not available. Horizons and faults were interpreted on the seismic sections as described in sections 4.4.2 and 4.4.3. Lithological information from previous interpretation by Vitel et al (2004) model permitted the identification of key geologic formations using time boundaries on the seismic sections and enabled the establishment of stratigraphic information of Lokichar the basin. Hydrocarbon prospective areas were determined based on the results of Loperot-1 well (Figure 5-16). Lithological information from Loperot-1 well was projected onto the vertical seismic display of seismic line TVK-127 since the well is near to the seismic line.

Interpretation for each seismic line was done separately to determine structural information, stratigraphic information and hydrocarbon traps and prospective areas.

CHAPTER FIVE

5.0. RESULTS AND DISCUSSIONS

5.1. Results

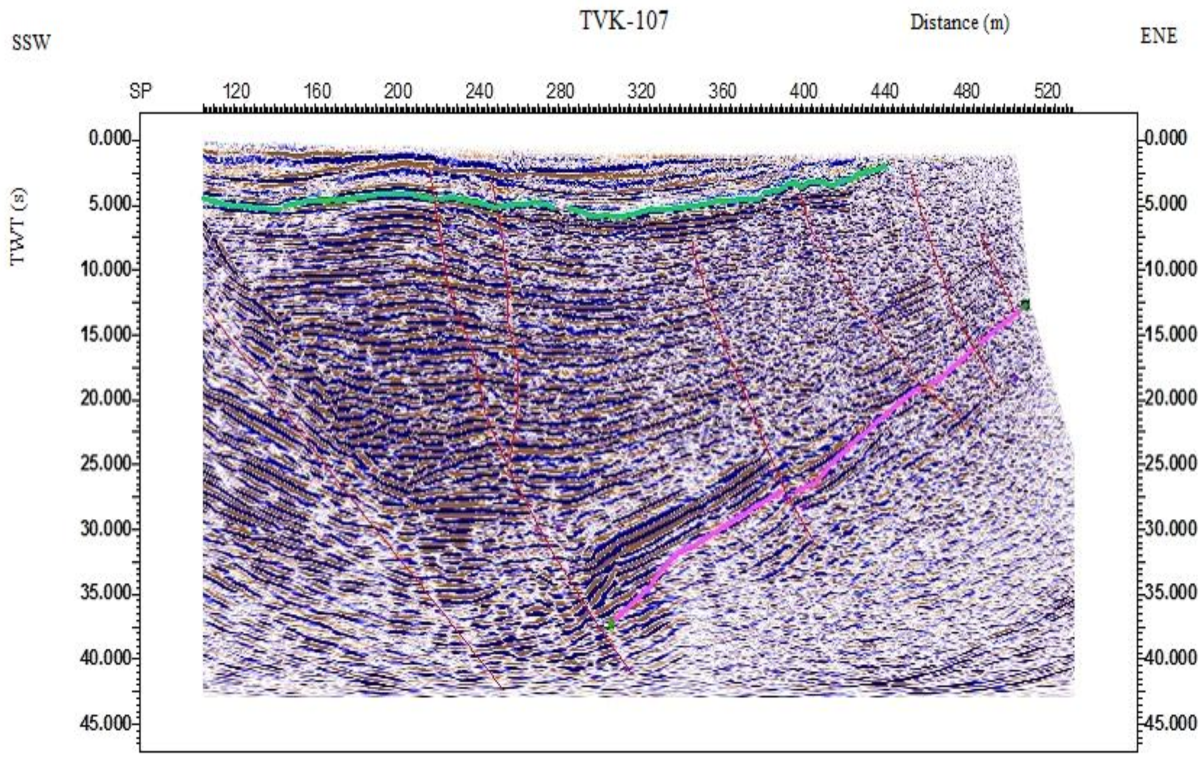

Figure 5-1: Interpreted vertical seismic display of line seismic TVK-107.

On the vertical seismic display of seismic line TVK-107, only two reflectors were easily recognized as shown in Figure 5-1. The lower reflector is distinct and represents the contact between Precambrian basement rocks and sedimentary sequences. Faults observable on the seismic section have been interpreted.

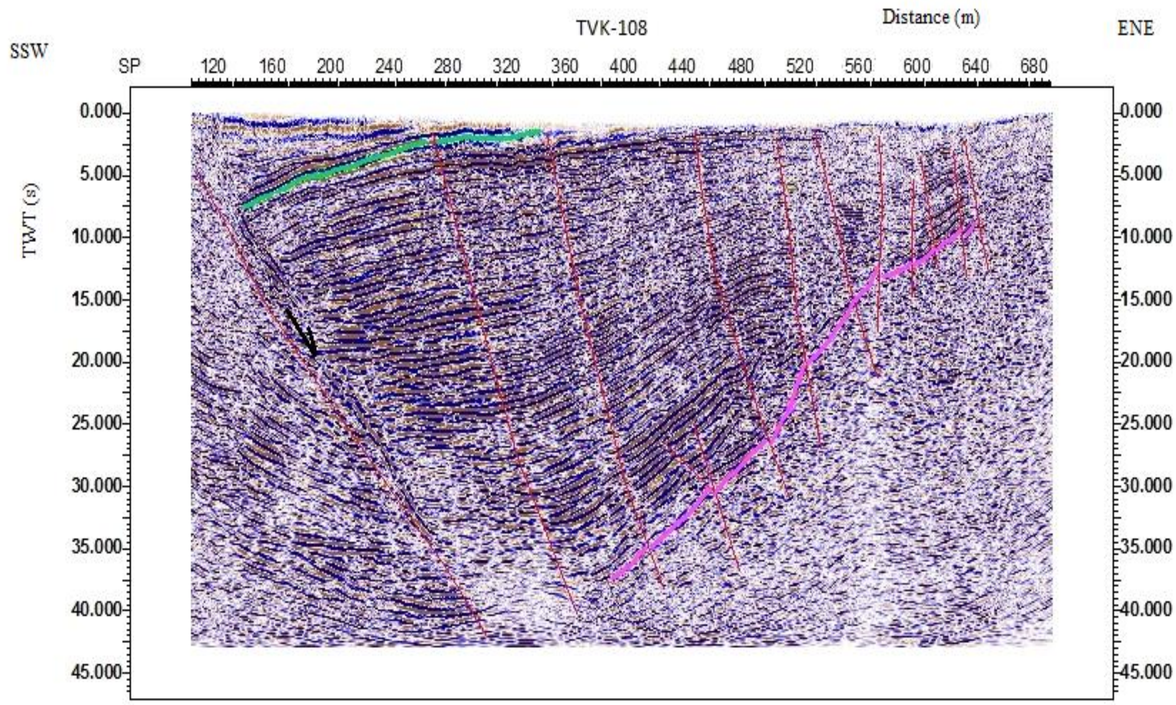

Figure 5-2: Interpreted vertical seismic display of seismic line TVK-108.

On the vertical seismic display of seismic line TVK-108 (Figure 5-2), only two reflectors were interpreted. The lower reflector representing the contact between Precambrian basement rocks and the sedimentary sequences was easily recognized. Recognizable faults on the seismic section were interpreted.

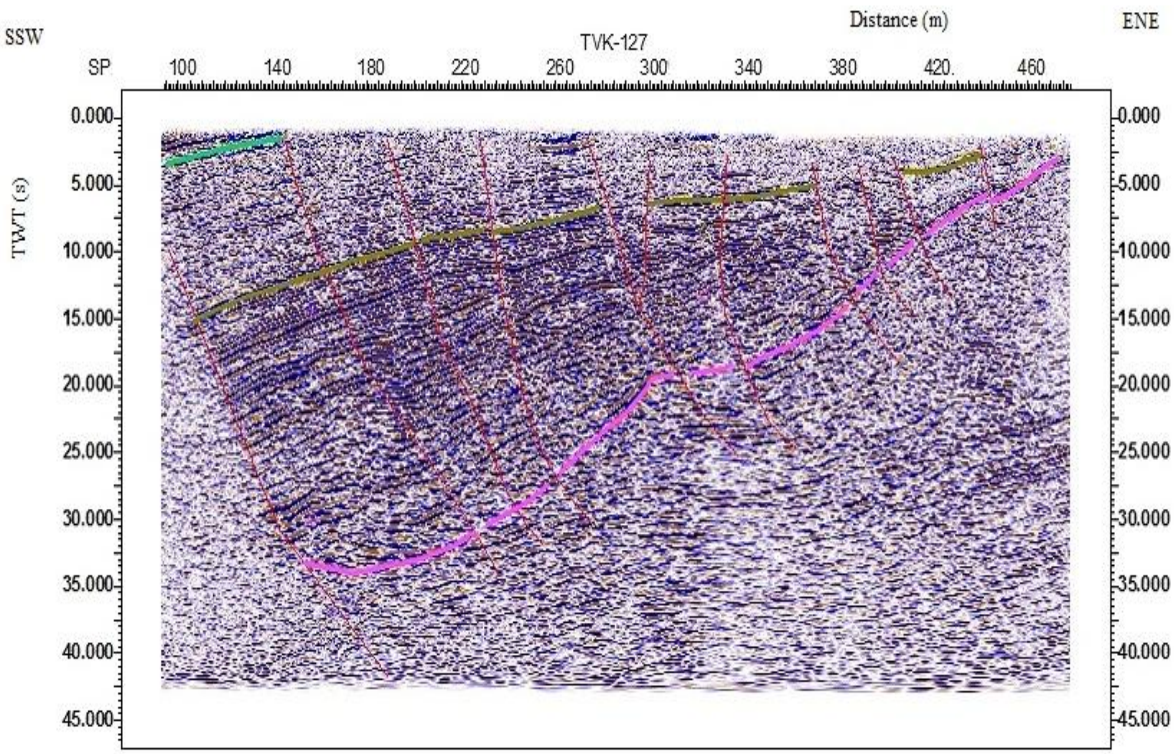

Figure 5-3: Interpreted vertical seismic display of seismic line TVK-127.

On the vertical seismic display of seismic line TVK-127, three reflectors were clearly identified and interpreted as shown in Figure 5-3. The lower reflector was easily recognized and represents the contact between basement rocks and sedimentary sequences. Based on the lithological information of Loperot-1 well (Figure 5-16) projected on to the seismic line TVK-127 (Figure 5-17), the middle reflector represents Loperot (Lokhone) shales. Observable faults on the vertical seismic display were also interpreted.

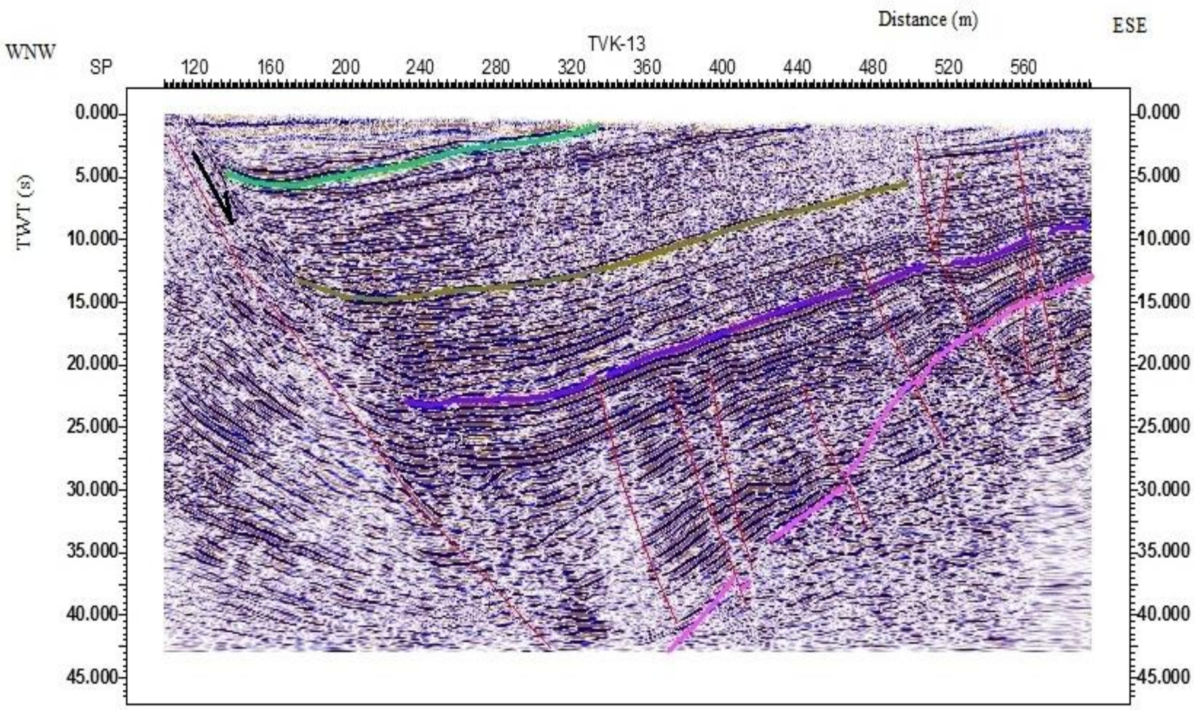

Figure 5-4: interpreted vertical seismic display of seismic line TVK-13.

On the vertical seismic display of seismic line TVK-13, four main reflectors were clearly identified and interpreted as shown in Figure 5-4. The lower reflector represents the contact between Precambrian basement rocks and the sedimentary sequences. The upper reflector could be representing the contact between volcanic rocks and Pliocene sediments.

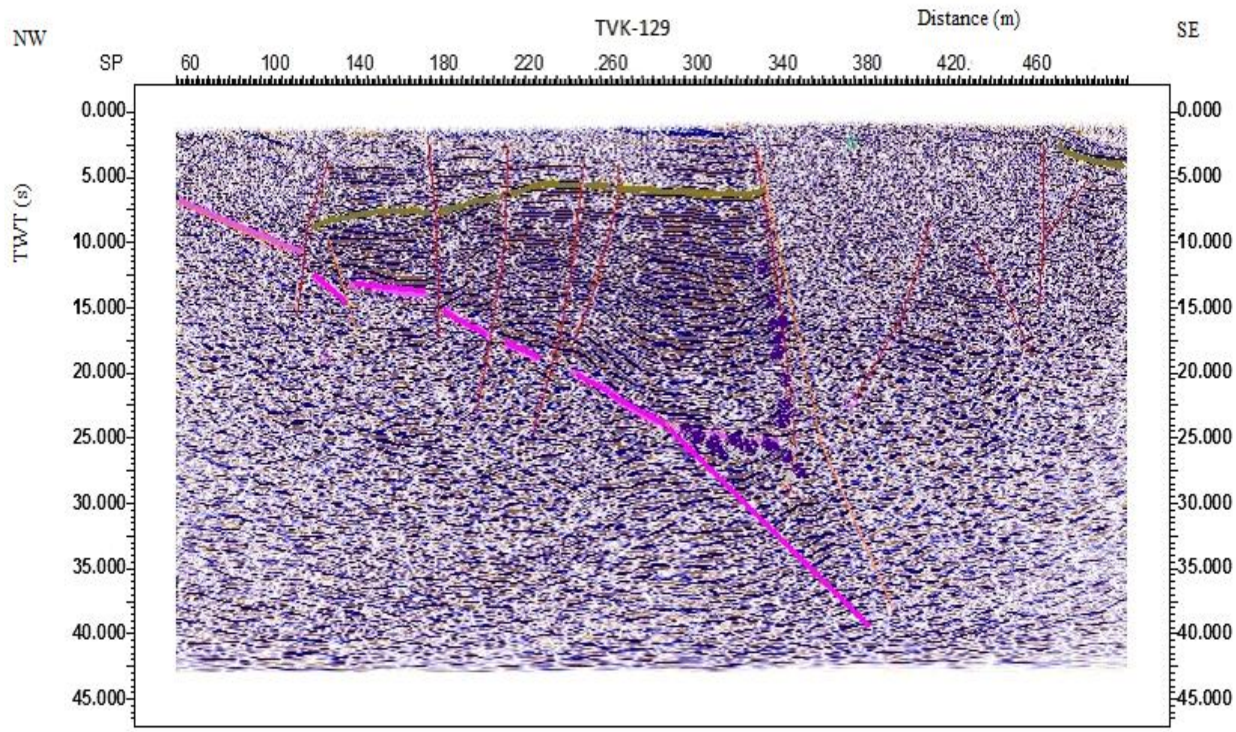

Figure 5-5: Interpreted vertical seismic display of seismic line TVK-129.

On the vertical seismic display of seismic line TVK-129, only two reflectors that were easily recognized were interpreted as (Figure 5-5). The lower reflector is distinct and represents the contact between Precambrian basement rocks and the sedimentary sequences. Minor faults observable on the seismic section were also interpreted.

5.2. Stratigraphy of Lokichar Basin

From the interpreted results shown in section 5.1, the configuration of seismic lines TVK-107, TVK-108 and TVK-127 was concluded to be the same as they appear similar on the vertical seismic displays. Seismic line TVK-13 has also a similar configuration (image) as the three seismic lines though it is oriented in different direction. The similarity in configuration of the vertical seismic displays of these seismic lines made it possible to identify and conclude the stratigraphy of Lokichar basin.

Results from a model by Vitel et al (2004) of seismic line TVK-107 (Figure 5-6) was used in this research to assign lithological information to the interpreted seismic sections beginning with seismic line TVK-107 as stated earlier. This information aided in determining the stratigraphic sequences and their geological time, which occur in Lokichar basin. Some geological units like alluvial fans which occur along the major bounding fault were determined and identified based on the Lambiase et al (1999) model of syn-rift facies distribution (Figure 5-12).

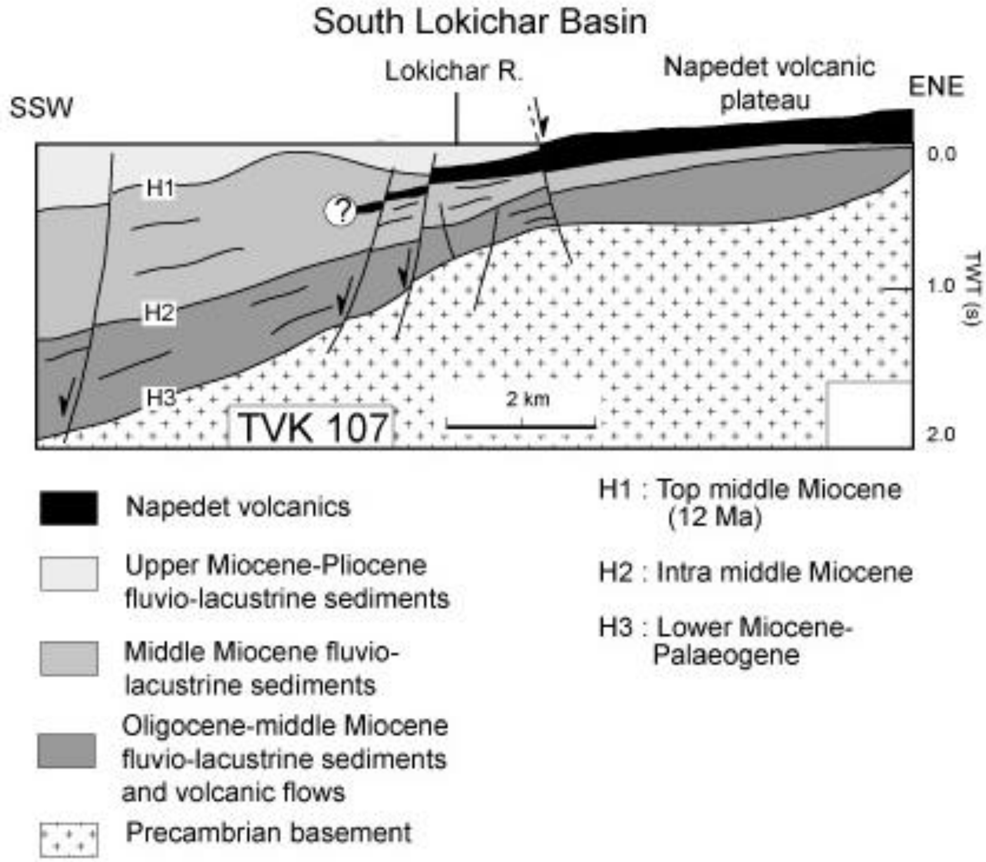

Figure 5-6: Previous interpretation of seismic line TVK-107 (Vitel et al., 2004).

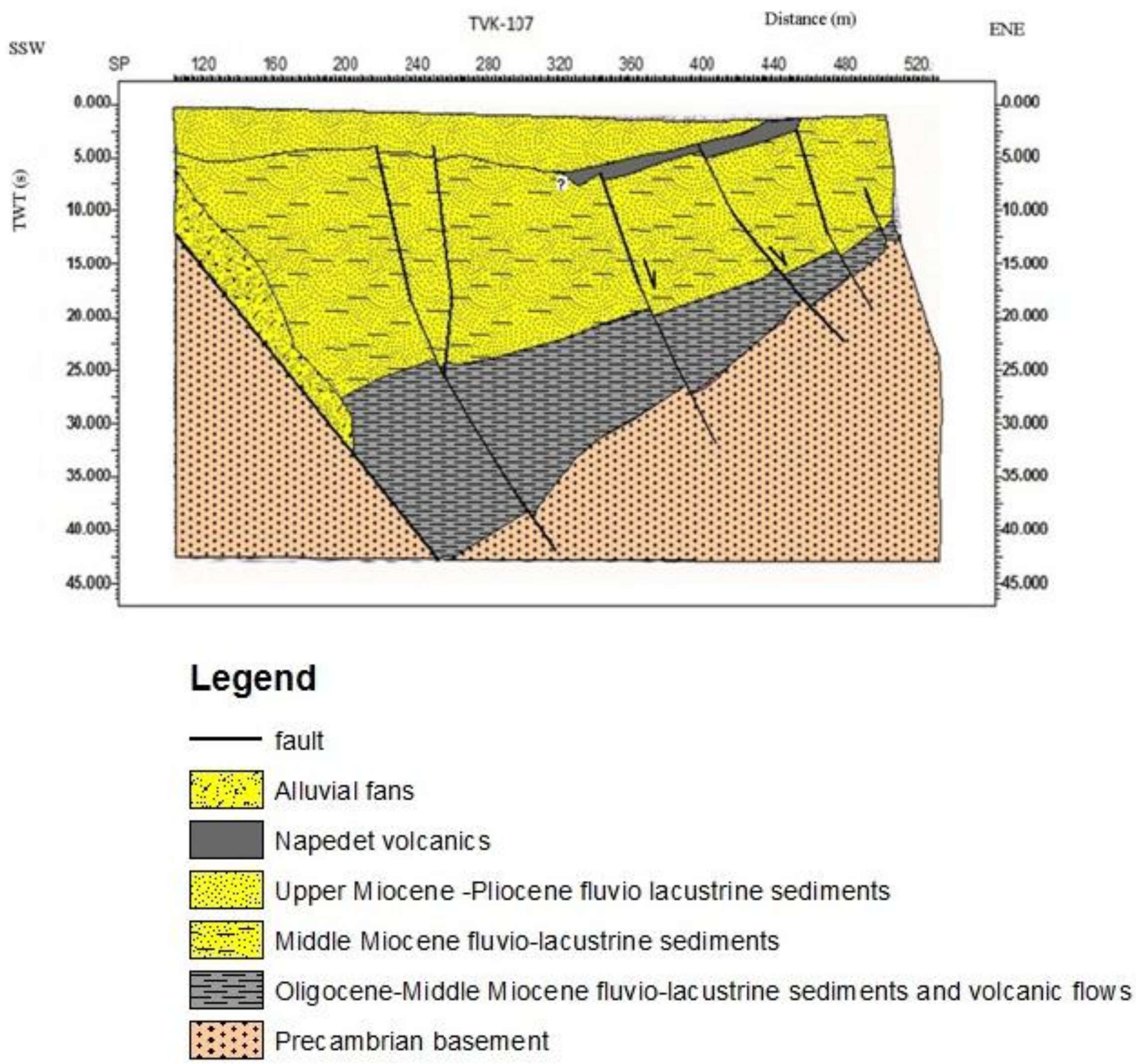

Figure 5-7: Interpreted vertical seismic display of seismic line TVK-107 showing rock stratigraphy and faults.

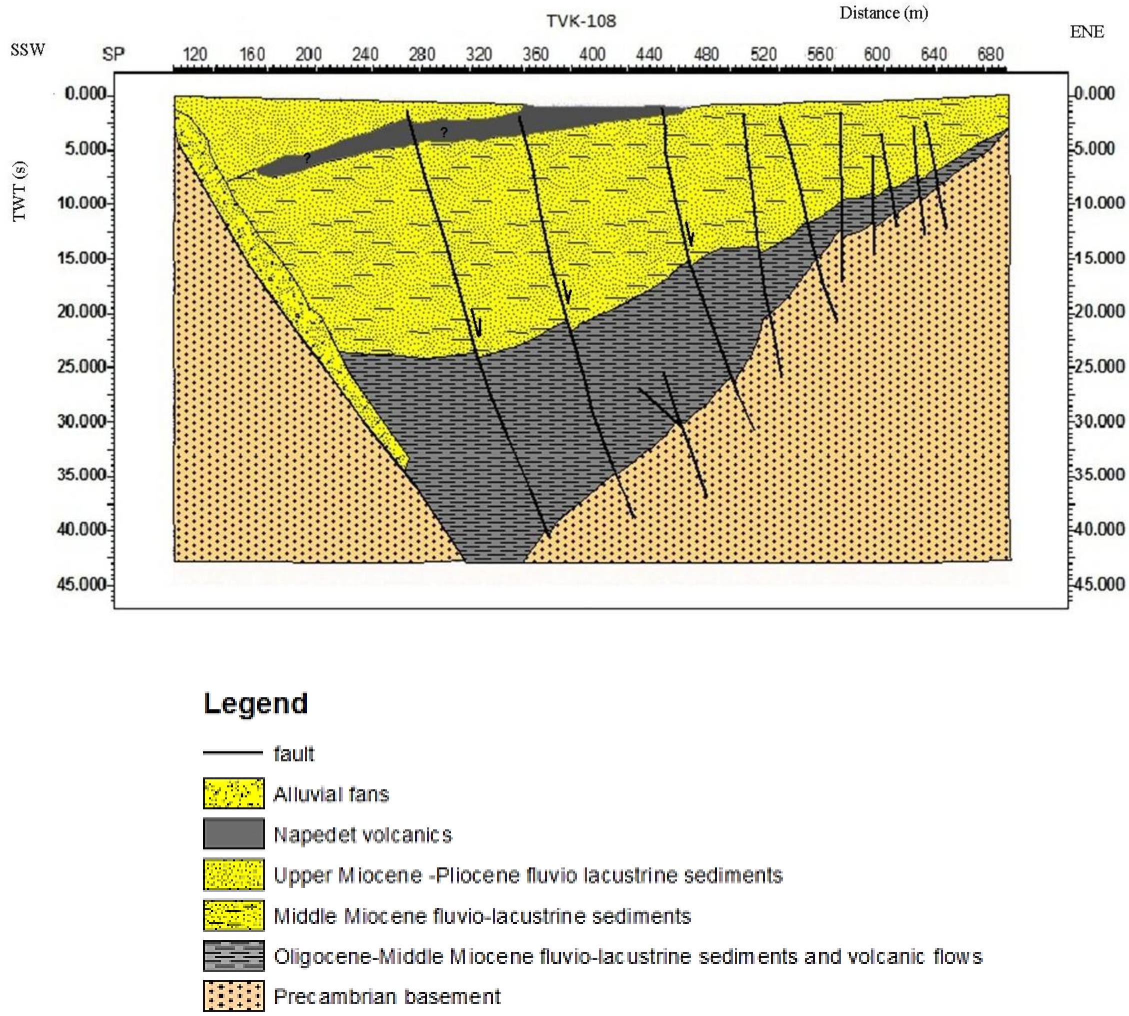

Figure 5-8: Vertical seismic display of seismic line TVK-108 showing rock stratigraphy and faults.

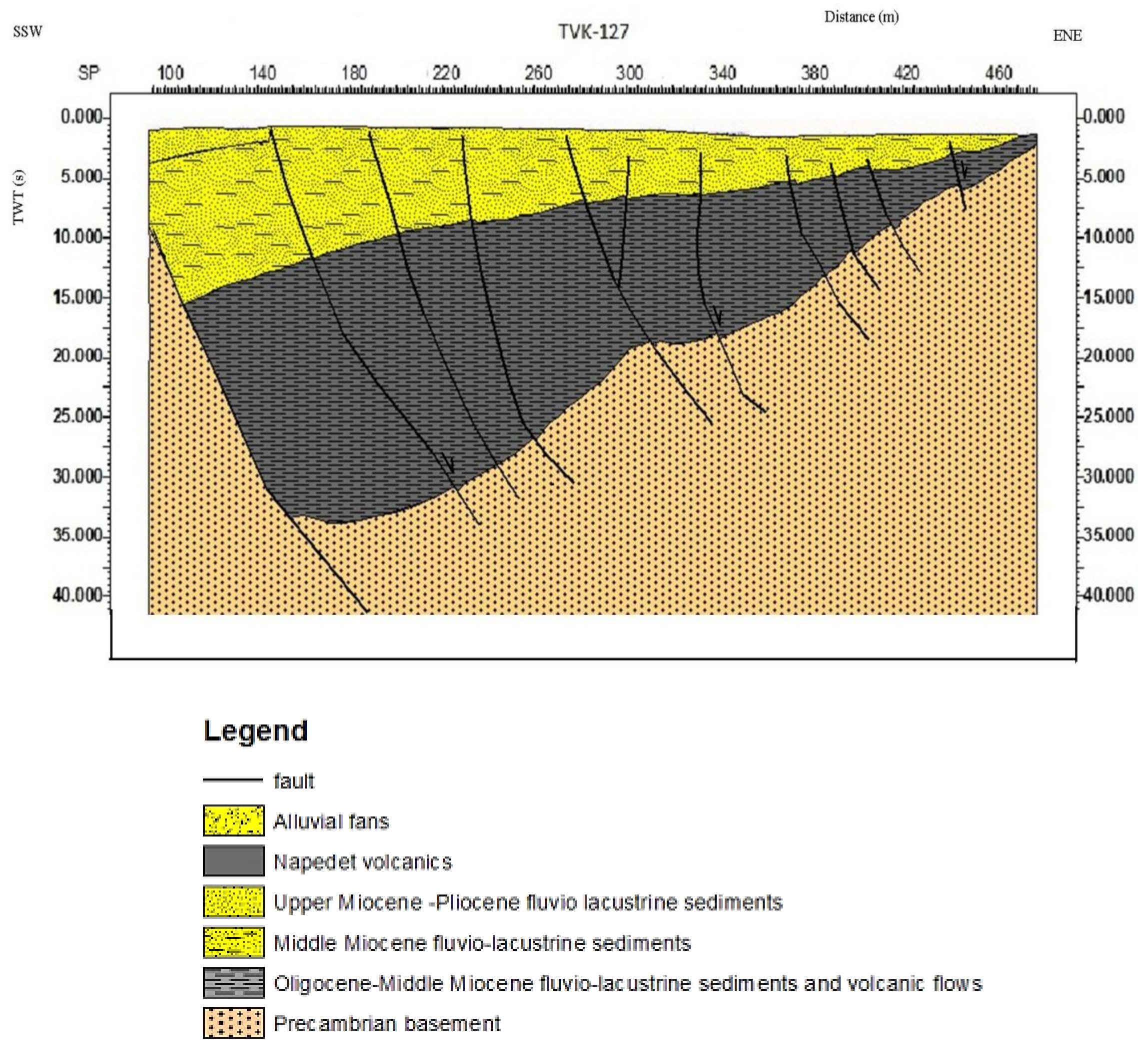

Figure 5-9: Vertical seismic display of seismic line TVK-127 showing rock stratigraphy and faults.

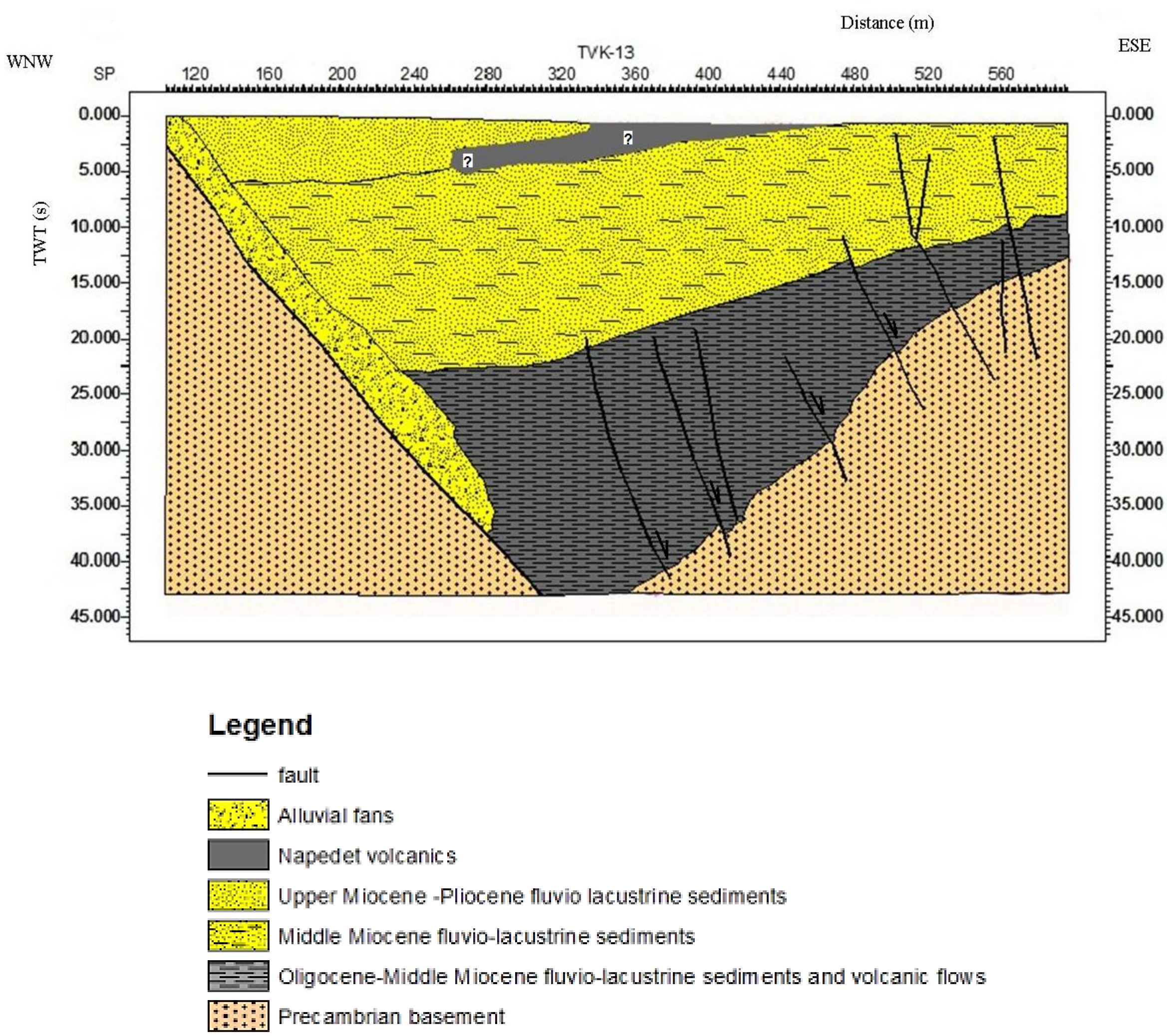

Figure 5-10: Vertical seismic display of seismic line TVK 13 showing rock stratigraphy and faults.

From the interpreted results of the four seismic sections of seismic lines TVK-107, TVK-108, TVK-127 and probably seismic line TVK-13 shown in Figures 5-1, 5-2, 5-3 and also Figure 5-4 simultaneously, stratigraphy of Lokichar basin was determined as shown in Figures 5-7,5-8, 5-9 and 5-10 simultaneously. This stratigraphy was determined based on the Vitel et al (2004) model (Figure 5-6) as stated. However, interpreted results were found to be contrary to that of Vitel et al (2004) model. In this research, only lithological information from the model was used. Therefore Lokichar basin was concluded to contain the following lithological units: Precambrian basement rocks, Oligocene-Middle fluvio-lacustrine sediments and volcanic flows, Middle-Pliocene fluvio-lacustrine sediments, Upper Miocene-Pliocene fluvio-lacustrine sediments, Napedet volcanics and alluvial fans.

5.2.1 Precambrian basement rocks

They form the base of Lokichar basin since they were observed on all the seismic vertical displays of the interpreted seismic lines. Basement rocks were found to be high on the western side and eastern side of the basin. These rocks are highly foliated or have undergone ductile shearing near Lokichar fault on seismic lines TVK-107, TVK-108 and TVK-13 shown in Figures 5-1, 5-2 and 5-4.

5.2.2 Oligocene-Middle fluvio-lacustrine sediments and volcanic flows

These sequences of rocks overlie the Precambrian basement rocks unconformably. Fluvio-lacustrine sediments in this formation could be responsible for generating hydrocarbons in the lower source rocks. These rock sequences thin up-dip towards the flexural edge of the basin. Figure 5-9 shows that the sediments could be exposed in the eastern side of the basin.

5.2.3 Middle Miocene fluvio-lacustrine sediments

Sediments in this formation could be the upper sources for hydrocarbons. They overlie Oligocene-Miocene fluvio-lacustrine sediments and volcanic flows. They appear to be very thick and extensive in Lokichar basin. These sediments are probably exposed in the eastern part of the basin as observed on the interpreted seismic sections.

5.2.4 Upper Miocene-Pilocene fluvio-lacustrine sediments

These sediments overlie the Middle Miocene sediments and could form future sources for hydrocarbons since they are lacustrine in nature. These rock sediments are exposed on the western side of Lokichar basin as shown in Figures 5-8, 5-9 and 5-10. They are extensive on the vertical seismic display of seismic line TVK-107 as shown in Figure 5-7.

5.2.5 Napedet volcanics

From the interpreted seismic lines Napedet volcanics occur as lava flows which form lenses. From the interpreted seismic sections, these volcanics could be outcropping at the surface towards the east of the basin as shown in Figure 5-7.

5.2.6 Alluvial fans

Alluvial fans were observed to occur along Lokichar fault. They appear to be sedimentary fill along the bounding fault. Seismic signature of alluvial fans is parallel to Lokichar fault. Alluvial fans were observed on vertical seismic display of seismic lines TVK-107, TVK-108 and TVK-13 shown in Figures 5-7, 5-8 and 5-10.

5.3. Structures in Lokichar Basin

5.3.1. Strata geometry

It was determined that the strata geometry of Lokichar basin is a syn-rift with sediments that are fault-bounded. The boundary fault has resulted in deposition and reorganization of sediments as shown in Figure 5-11. The primary controls on the strata geometry has been described by Fiebel (2011) to be the interplay between accommodation space, the product of subsidence, and sedimentation working to fill or overwhelm the subsiding basin.

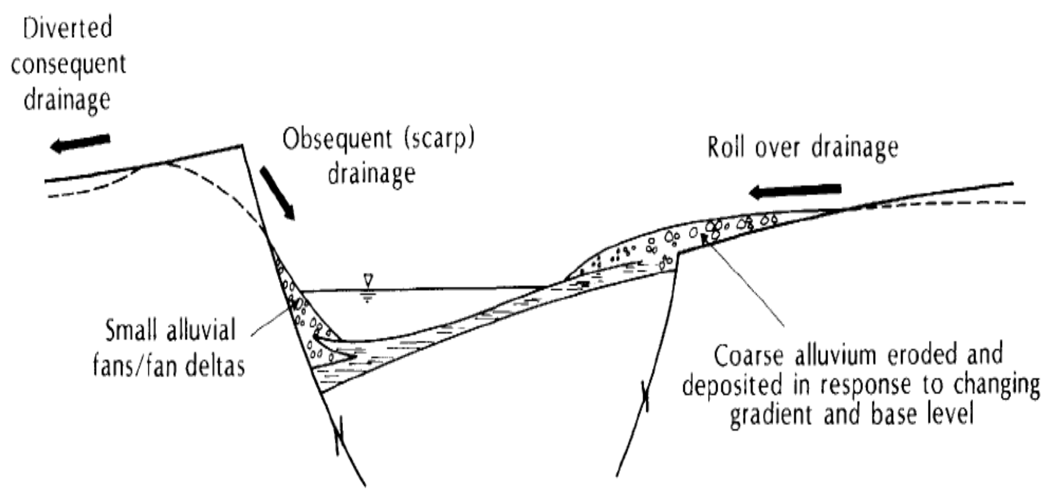

Figure 5-11: Active Boundary fault that results into reworking of sediments (Frostick & Reid 1987).

From the vertical seismic displays of all the interpreted seismic lines, it was determined that the sedimentary sequences with Lokichar basin have an asymmetric cross-section. This is because deposition occurs while subsidence continues along the bounding fault of an evolving half graben (Lambiase et al., 1999). Depositional units thicken towards the bounding fault and thin to the up-dip flexural edge as illustrated in Figure 5-12. Basement is higher on the western and eastern side of the basin.

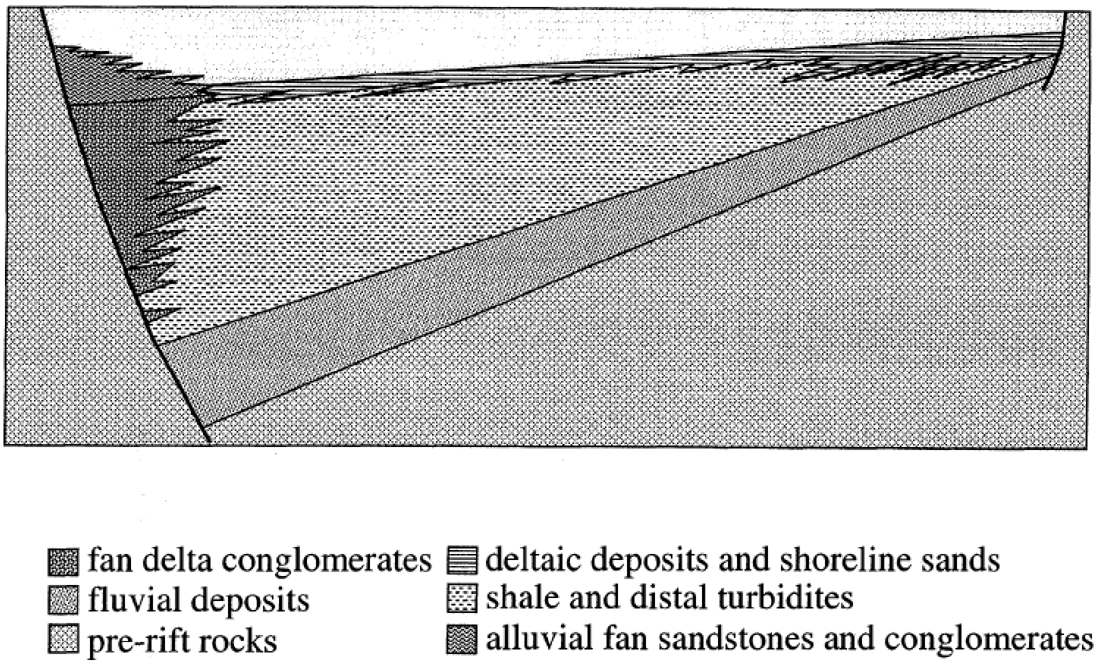

Figure 5-12: Idealized cross-section of syn-rift facies distribution (Lambiase et al., 1999).

5.3.2. Faults

It was confirmed from the interpreted seismic lines that the basin has a major bounding fault called Lokichar fault in the western side that dips towards the eastern side. On the Kingdom Suite base map a time slice of Lokichar fault appears as shown in Figure 5-13. Extrapolated time contours of the fault suggest that the fault could be deeper on seismic lines TVK-107 and TVK-108 since they almost cut across the fault. Vertical seismic display of seismic line TVK-13 is oblique to Lokichar fault.

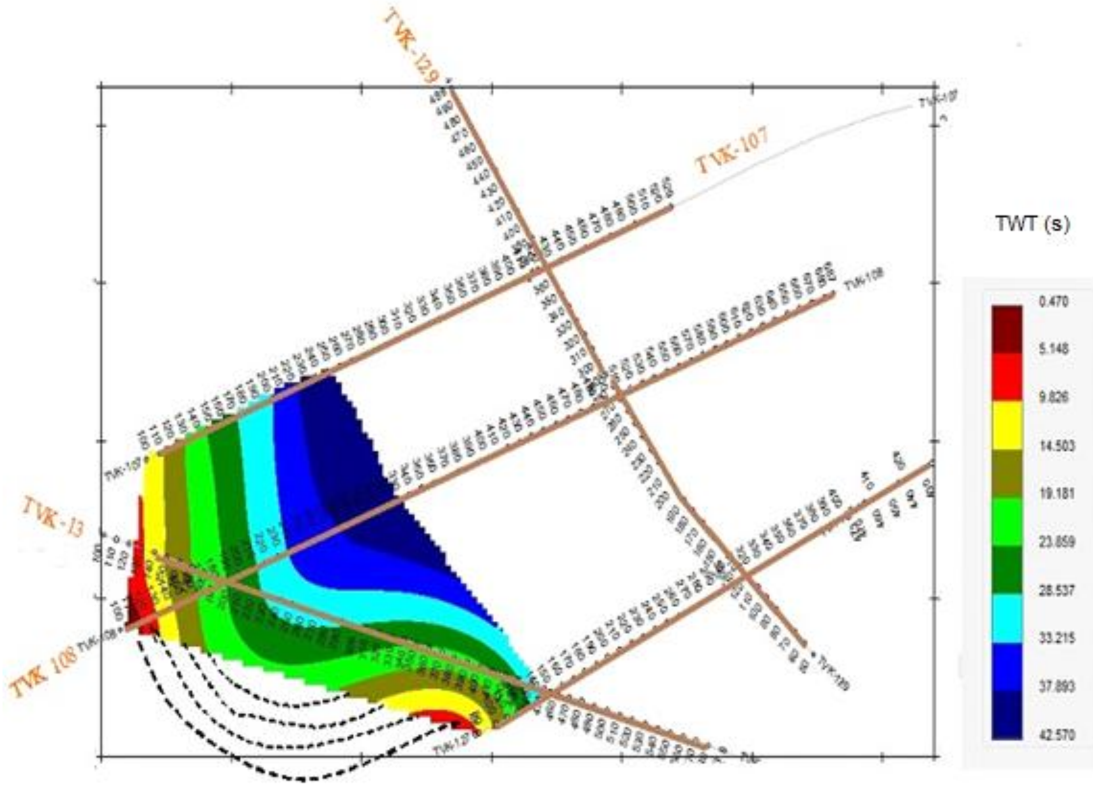

Figure 5-13: Time slice section showing orientation of Lokichar fault on the seismic sections.

Lokichar Fault has been described by Thuo (2009) to be listric in nature with no present-day topographic expression but the fault was found to be a generally a normal low angle fault on the vertical seismic display of seismic line TVK-107 (Figure 5-15). Lokichar fault was observed on the vertical seismic displays of seismic lines TVK-13, TVK-108, TVK-107 and TVK-127. Lokichar basin is highly faulted with a series of other faults which were observed on the vertical seismic displays of all the seismic lines. Most of the other faults are normal high angle faults while some are listric in nature (Figures 5-14 and 5-15). It was observed that majority of the other faults are trending parallel to the main basin bounding Lokichar fault.

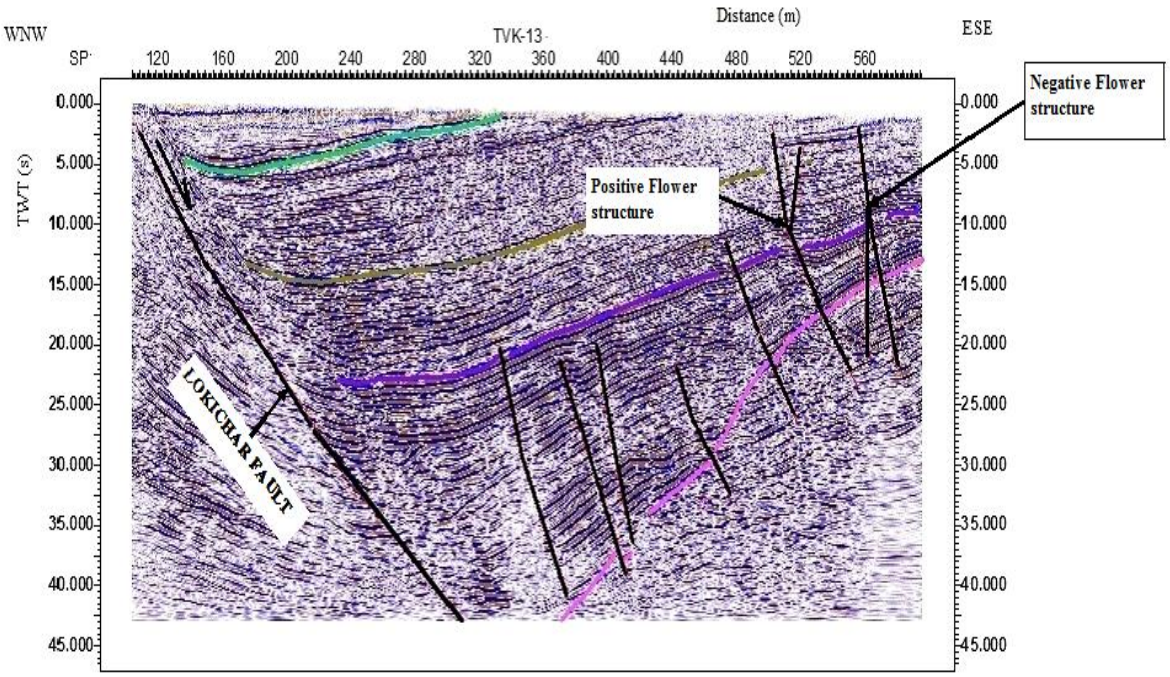

Figure 5-14: Interpreted vertical seismic display of seismic line TVK-13 showing Lokichar fault and flower structures.

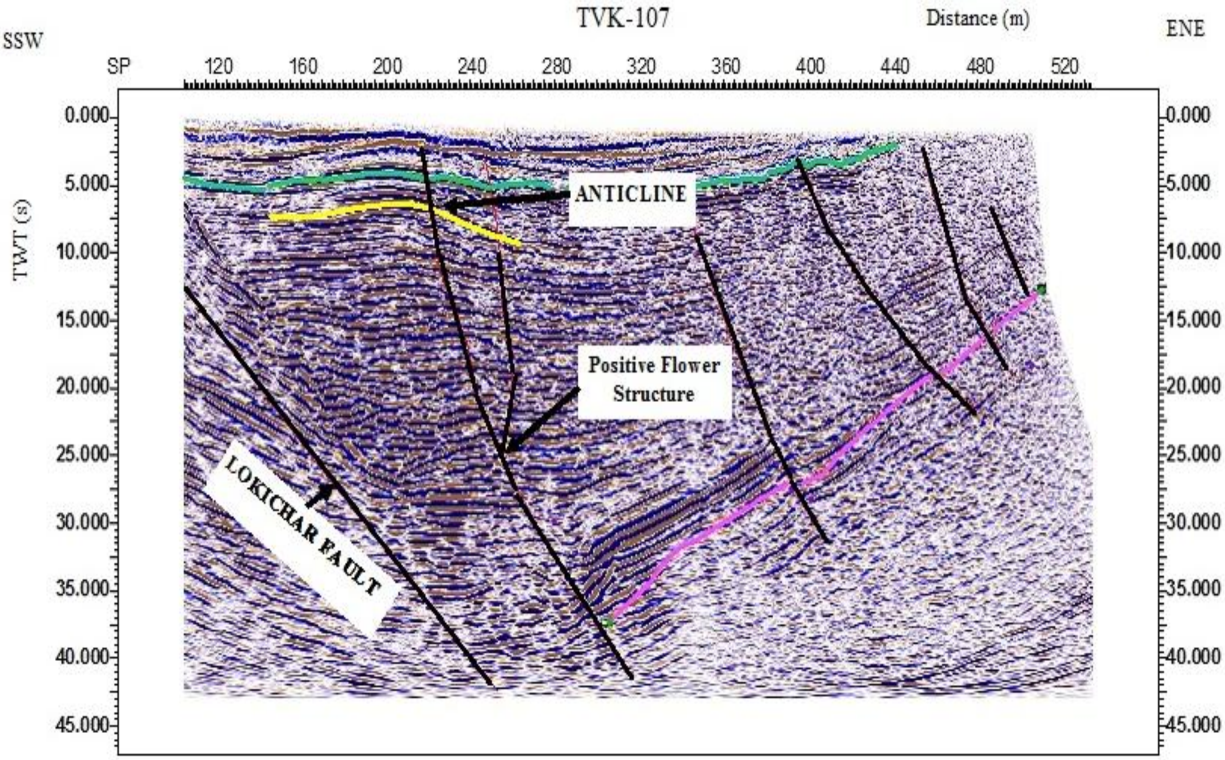

Figure 5-15: Interpreted vertical seismic display of seismic line TVK-107 showing structures.

5.3.3. Flower structures

Interpreted results have revealed the existence of positive and negative flower structures within Lokichar basin. Positive and negative flower structures were observed on the vertical seismic displays of seismic lines TVK-13, TVK-107, TVK-108 and TVK-127. Positive and negative flower structures are illustrated on Figure 5-14. Flower structures were previously interpreted in Turkana rift and they also occur in the Albertine Graben. In Lokichar basin, flower structures are commonly associated with transfer faults (Dunkelman et al., 1989). Seismic sections showing flower structures in the Albertine Graben in Uganda are shown in Appendix B.

5.3.4. Folding

As evidenced from the interpreted vertical seismic displays, folding is minimal in Lokichar basin. Folding is represented by presence of an anticline on the vertical seismic display of seismic line TVK-107 shown in Figure 5-15. Folding in the Turkana rift has been described to be as a result of extension and inversion of extensional structures (Le Gall et al., 2005).

5.4. Hydrocarbon traps and prospective areas

The major hydrocarbon traps in Lokichar basin are structural in nature. Hydrocarbons are trapped at fault closures and at fold anticlines. The major types of traps observable on all the vertical seismic displays are the fault closures. However, on the vertical seismic display of seismic line TVK-107, an anticline formed as a result of folding could be responsible for hydrocarbon trapping as shown in Figure 5-18. The second reflector shown on Figure 5-17 is acting as source for hydrocarbon generation and seal for the migrating hydrocarbons from the lower sources.

There is abundant accumulation of thick sequences of organic oil-prone mudstones and shales in Lokichar basin as evidenced from the results of Loperot-1 well. However, it was not possible to determine direct hydrocarbon indicators in the reservoir and their signatures on the vertical seismic displays of the seismic lines since the resolution of the seismic data was very low.

Determination of hydrocarbon prospective areas on the vertical seismic sections was done based on lithological information of Loperot-1 (Figure 5-16) plus stratigraphic and structural interpretations carried out in this research. This included availability of hydrocarbon source rocks in the fluvio-lacustrine sediments and hydrocarbon traps (Figures 5-16 and 5-17).

Source rocks include many lacustrine shales deposited in rift lake which are credited with sourcing numerous hydrocarbon accumulations worldwide (Lambiase et al., 1999). In terms of source rock potential, the presence of a source rock in the Lokichar basin is not a critical question (Thuo 2009). Lokichar Basin contains lacustrine shales, which exhibit many of the characteristic features of source rocks developed in continental rifts (Talbot et al., 2004).

The two black shale intervals encountered by the Loperot-1 well (Figure 5-16) have been described as good quality source rocks. The upper Lokhone Shale Member still has relatively high HI (Talbot et al., 2004). It is thus probable that significant volumes of liquid hydrocarbons have already been generated from this unit, which still has considerable generative potential (Talbot et al., 2004). On the vertical seismic displays of seismic lines TVK-127 and TVK-107, recommended target sites for drilling which could possibly penetrate two zones of hydrocarbon reservoirs have been illustrated in Figures 5-17 and 5-18.

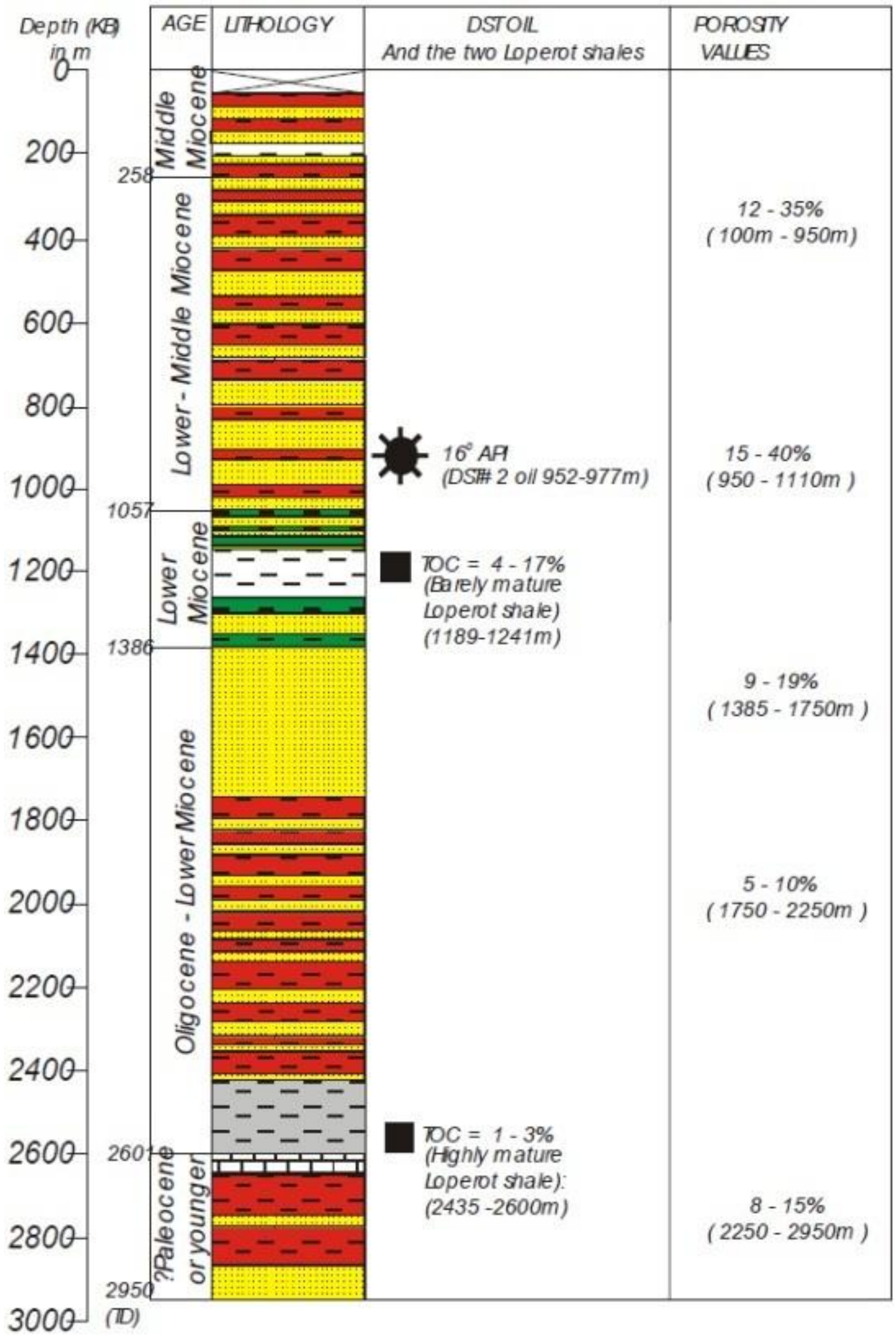

Figure 5-16: Loperot-1 well lithological information (Heya 2011).

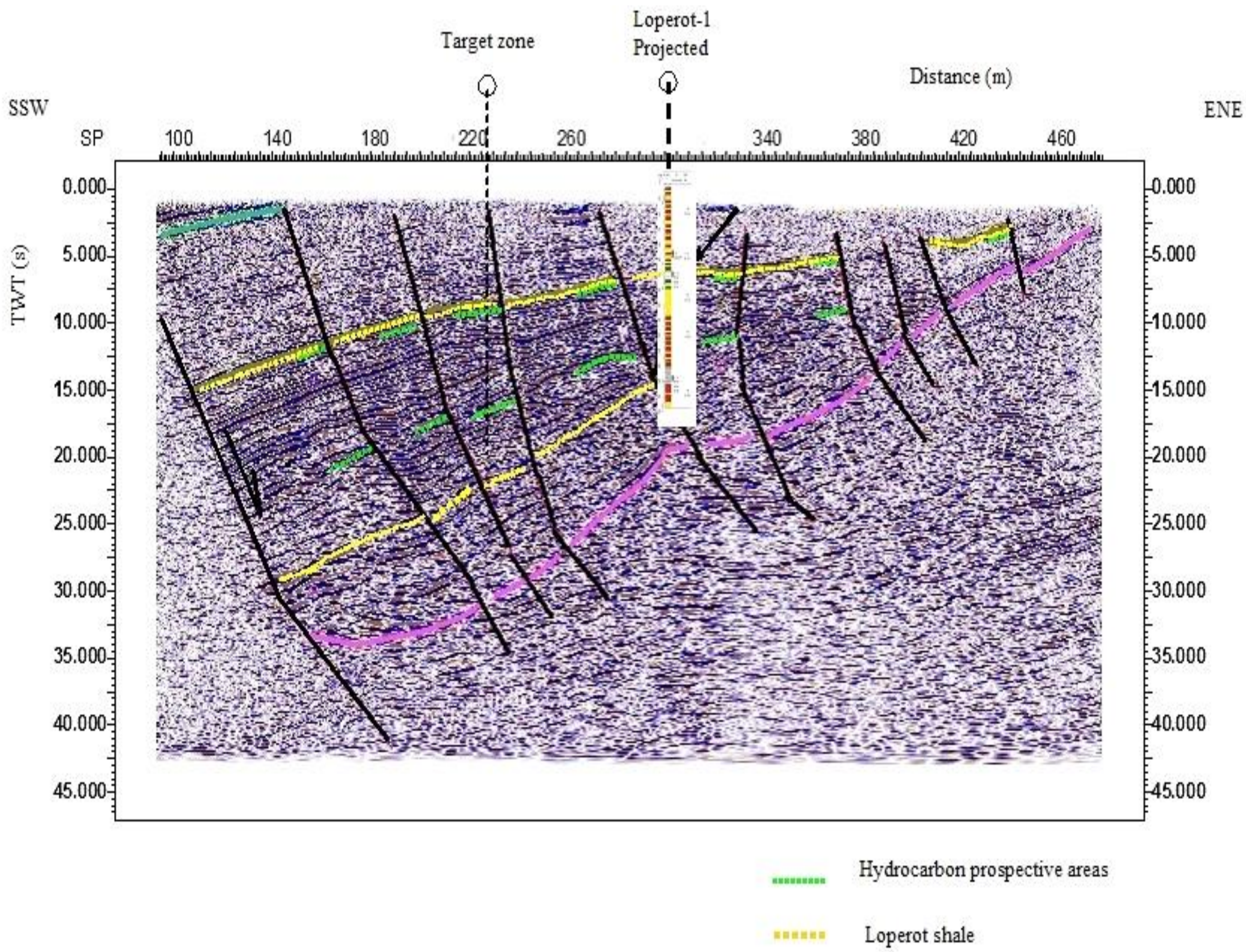

Figure 5-17: Seismic line TVK-127 showing hydrocarbon prospecting areas and target site for drilling. Loperot-1 well is projected on the seismic line.

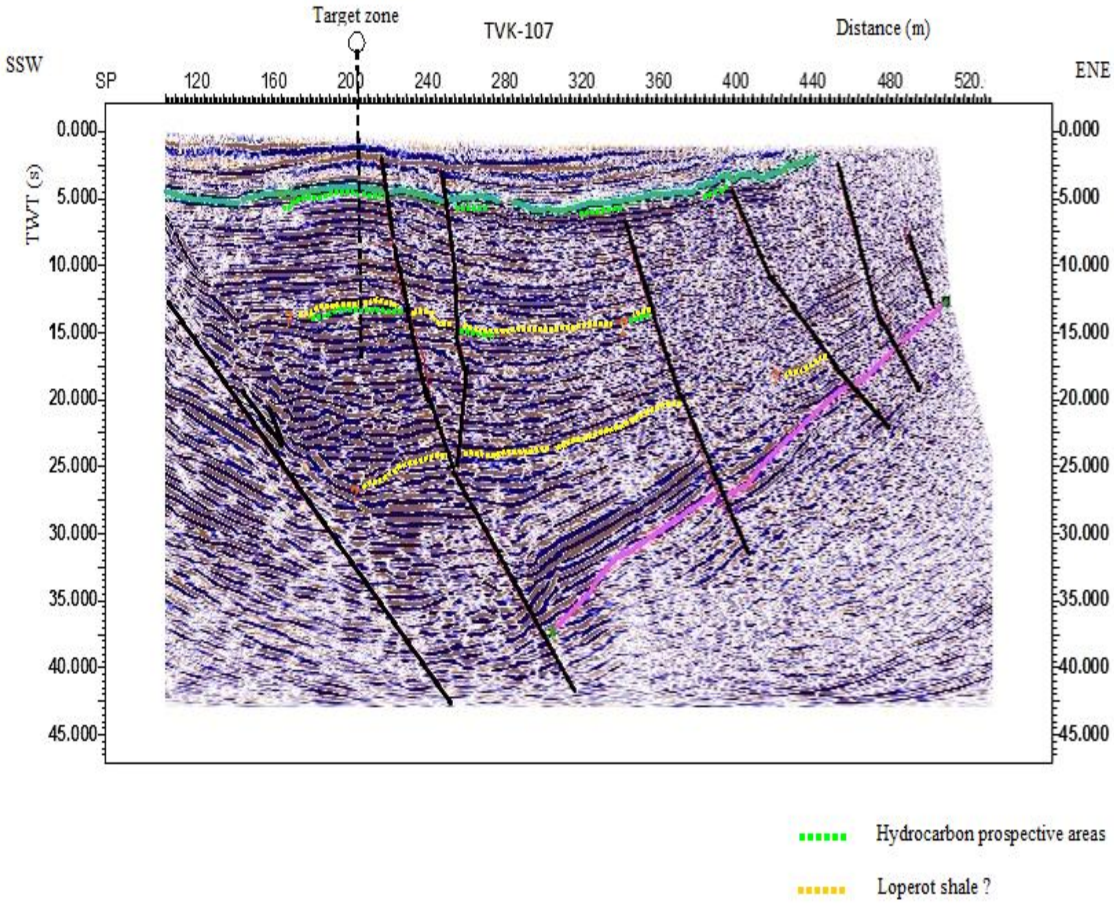

Figure 5-18: Seismic line TVK-107 showing possible hydrocarbon traps, prospective areas and target site for drilling.

CHAPTER SIX

6.0. CONCLUSIONS AND RECOMMENDATIONS

6.1. Conclusions

The main purpose of this research was to determine the sub-surface structures with the goal of identifying and delineating possible hydrocarbon prospective areas. From the sub-surface information obtained by interpretation of the five seismic sections, it has been confirmed that there exists a half-graben structure in Lokichar basin as described by previous researchers.

Results have also confirmed that sedimentation in Lokichar basin was controlled by the basin geometry and the marginal bounding fault. The fault created accommodation zone for accumulation sediments. Sediments were found to be thick at the western side on the bounding fault and thin out towards the eastern side of the basin. Therefore the sedimentary sequences have an asymmetrical cross-section.

The contact between basement rocks and sedimentary sequences within Lokichar basin was determined and was found to be high on the western and eastern side of the basin. Basement reflectors were clearly distinguishable on all the vertical seismic displays of the interpreted seismic lines. Vertical displays of seismic lines TVK-13, TVK-108 and TVK-107 have confirmed that the basement rocks could be highly foliated or have undergone ductile shearing towards Lokichar fault.

Structurally, it was confirmed that Lokichar basin has a major bounding fault called Lokichar fault at the western side dipping towards the east. Lokichar fault was observed on vertical seismic displays of 4 seismic lines to be a normal low angle fault. A series of other faults were also interpreted on the vertical seismic displays. Results have also shown that the other faults are either high angle or listric in nature. They almost trend in the same manner as the major basin bounding fault. Some faults in Lokichar basin branch forming positive and negative flower structures.

Folding of sedimentary sequences is evident in Lokichar basin though on a minimal scale. Folding is represented by presence of an anticline on the vertical seismic display of seismic line TVK-107. In Lokichar basin, folding could be as a result of extension and inversion of extensional structures.

It was determined that fault closures and fold anticlines could be responsible for hydrocarbon trapping in Lokichar basin hence forming the possible hydrocarbon prospecting areas. The upper Lokhone (Loperot) shale could be acting as a source for hydrocarbons and also as a seal for hydrocarbons from the lower shales.

6.2. Recommendations

From the findings of this research, it is recommended that seismic data interpretation should be tied to well log data to control time to depth migration and give accurate lithological information representing the reflectors.

Seismic tomography of these interpreted seismic lines is highly recommended to get a clear picture representative of the subsurface and compare it these findings.

It is also recommended that these seismic interpretation results are integrated with findings from other geophysical prospecting methods such gravity, magnetic and electrical resistivity.

Use more recently acquired seismic data is highly recommended since seismic data acquisition techniques have improved. 3D seismic data is also recommended as it will give a good image of the basin.

Target zones for drilling have been estimated and therefore recommended on seismic lines TVK-127 and TVK-107.

REFERENCES

Admasu, F., 2008. A Stochastic Method for Automated Matching of Horizons across a Fault in 3D Seismic Data Dissertation. *Master of science thesis*, p.131.

Arthur, M. C., 1937. Physiography of the region to the west and south-west of Lake Rudolf. *Royal Geographical Society*, 89(2), pp.97–118.

Bartucz, D., 2009. Exploration of Geothermal Systems with Petrel Modeling Software. *School for Renewable Energy*, p.69.

Bjorlykke, K., 2010. Sequence Stratigraphy, Seismic Stratigraphy and Basin Analysis. *Environments*, pp.235–251. Available at: http://www.springerlink.com/index/10.1007/978-3-642-02332-3 [Accessed July 28, 2011].

Borgos, H.G., Skov, T. & Sønneland, L., 2005. Automated Structural Interpretation Through Classification of Seismic Horizons. *Schlumberger Stavanger Research*, pp.90–106.

Dunkelman, T.J., Rosendahl, B.R. & Karson, J.A., 1989. Structure and stratigraphy of the Turkana rift from seismic reflection data. *Journal of African Earth Sciences*, 8(2-4), pp.489–510. Available at: http://linkinghub.elsevier.com/retrieve/pii/S0899536289800417.

Feibel, C.S., 2011. A Geological History of the Turkana Basin. *Evolutionary anthropology*, 216, pp.206–216.

Frostick, L. E. & Reid, I., 1987. Tectonic control of desert sediments in rift basins ancient and modern. *Geological Society of London*, 35(Special publication), pp.53–68.

Fuchs, V.E., 1939. The geological history of the Lake Rudolf Basin, Kenya Colony. *Royal Society Publishing*, 229(560), pp.219–274.

Fugro, 2007. Seismic data Processing. *Fugro Seismic Imaging Pty Ltd-Report for Origin Energy*, 61(July), p.55.

Gadallah, M.R. & Fisher, R., 2009. Seismic Interpretation. In *Exploration Geophysics*. Berlin, Heidelberg: Springer Berlin Heidelberg, pp. 149–221. Available at: http://www.springerlink.com/index/10.1007/978-3-540-85160-8 [Accessed December 2, 2011].

Grove, A.T., 1986. Geomorphology of the African Rift System. *Geological Society, London, Special Publications*, pp.9–16.

Hager, C.R., 2009. Seismic interpretation of Atokan strata using 3D seismic inversion data, Wilburton gas field, Arkoma Basin, southeastern Oklahoma. *Msc thesis, Oklahoma State University*, p.109.

Heya, M., 2011. Overview of Petroleum Exploration in Kenya. *Presentation to the 5th East African Petroelum Conference and exhibition by Ministry of energy (Kenya)*, p.31.

Joubert, P., 1966. Geology of the Loperot area. *Geological Survey of Kenya*, (Report No. 74), p.51.

Kearey, P., Brooks, M., and Hill, I., 2002. An introduction to geophysical exploration. *Blackwell Science Publishing*, (Third Edition), p.281. Available at: http://scholar.google.com/scholar?hl=en&btnG=Search&q=intitle:An+Introduction+to+Geophysical+Exploration#0 [Accessed May 28, 2012].

Keqiang, W., 2007. Comparison between Kenya Tertiary Rift and Liaodong Bay Depression. In *11th Africa Oil & Gas, Trade & Finance Conference and Exhibition*. p. 35.

Khan, M.A. & Swain, C.J., 1978. Geophysical investigations and the Rift Valley geology of Kenya. *Geological Society, London, Special Publications*, 6(1), pp.71–83. Available at: http://sp.lyellcollection.org/cgi/doi/10.1144/GSL.SP.1978.006.01.07 [Accessed April 18, 2012].

Lambers, E.J.T., 1993. Prospectivity Review of Block 10BB, Kenya. *Shell Exploration & Production Kenya B.V.*, p.21.

Lambiase J. J., Morley, C. K., White R. S., Watts, A. B., Bowler, D., & Kusznir, N., 1999. Hydrocarbons in rift basins: the role of stratigraphy. *Royal Society Publishing*, 357(1753), pp.877–900.

Le Gall, B., Vitel, W., and Morley, C.K., 2005. Inversion tectonics during continental rifting: The Turkana Cenozoic rifted zone, northern Kenya. *Tectonics*, 24(2), pp.1–17. Available at: http://www.agu.org/pubs/crossref/2005/2004TC001637.shtml [Accessed December 21, 2011].

Mariita, N.O., 2003. An integrated geophysical study of the northern Kenya structure. Implications for geothermal energy prospecting for Menengai area. *ETD Collection for University of Texas, El Paso*, (AA13118500), p.204.

Marillier, F., Eichenberger, U., Sommaruga, A., 2006. Seismic synthesis of the Swiss Molassw Basin. *Schweizerische Geophysilaische Kommission SGPK, Annual Report.*, pp.1–16.

Mondol, H.Z., 2010. Seismic Exploration. *Petroleum Geoscience*, pp.375–402. Available at: http://www.springerlink.com/index/10.1007/978-3-642-02332-3 [Accessed July 28, 2011].

Morley, C.K., 1995. Developments in the structural geology of rifts over the last decade and their impact on hydrocarbon exploration. *Geological Society, London, Special Publications*, 80(1), pp.1–32. Available at: http://sp.lyellcollection.org/cgi/doi/10.1144/GSL.SP.1995.080.01.01 [Accessed April 11, 2012].

Morley, C. K., Wescott, W. A., Stone, D. M., Harper, R. M., Wigger, S. T., & Karanja, F.M., 1992. Tectonic evolution of the northern Kenyan Rift. *Journal of Geological Society, London*, 149(Arambourg 1933), pp.333–348.

Nilanjan, R., 2008. Analysis and Interpretation 2D seismic data over the Ancona gas storage facility, Illinois, using Petrel visualization software. *MSc thesis Wright State University*, p.73.

NOCK, 1987. Geological map of Kenya. *National Oil Corporation of Kenya*.

Olang, M.O., 1979. Vegetation cover assessment in Turkana District, Kenya. *Kenya Rangeland Econoligical Monitoring Ubit, Nairobi, Kenya*, p.24.

PEPD, 2009. Petroleum potential of the Albertine graben. *Petroleum Exploration and Production Department , Ministry of Energy and Mineral Development. Republic of Uganda. Brochure*, p.20.

Ray, D. S. and Mayor, S., 2006. Syn-rift sequences through transfer zones–thrust Area for future exploration in Cambay Basin, Western India. *6th International Conference & Exposition on Petroleum Geophysics*, (c), pp.957–962.

Rhemtulla, S., 1970. The South Turkana Expedition: Scientific Papers III. A Geological Reconnaissance of South Turkana. *The Royal Geographical Society*, 136(1), pp.61–73.

Schuck, A and Lange, G., 2007. 4 . 6 Seismic Methods. *Environmental Geology, 4 Geophyics*, pp.337–402.

Schuster, G.T., 2010. Basics of Exploration Seismology and Tomography. *Stanford Mathematical Geophysics Summer School Lectures*, p.20.

Scintrex, 1996. Magnetic Applications Guide. *SCINTREX Limited*, p.56.

Shackleton, R.M., 1978. Structural development of the East African Rift system. *Geological Society, London, Special Publications*, 6(1), pp.19–28. Available at: http://sp.lyellcollection.org/cgi/doi/10.1144/GSL.SP.1978.006.01.04 [Accessed March 30, 2012].

SMT, 2012. Geophysical and Geological interpretation System. *Seismic Micro Technology, Inc*, p.43. Available at: www.seismicmicro.com.

Talbot, M.R., Morley, C.K., Tiercelin, J.J., Le Hérissé, A., Potdevin, J.L., Le Gall, B., 2004. Hydrocarbon potential of the Meso-Cenozoic Turkana Depression , northern Kenya. II. Source rocks: quality, maturation, depositional environments and structural control. *Marine and Petroluem Geology*, 21, pp.63–78. Available at: www.elsier.com/locate/marpetgeo.

Telford, W. M., Geldart, L. P. and Sheriff, R.E., 1990. Applied Geophysics. *Cambridge University Press*, p.784.

Thuo, P., 2009. Stratigraphic, petrographic and diagenetic evaluation of Cretaceous/ Paleogene potential reservoir sandstones of western Turkana, Kenya. Implications on the petroleum potential of northwestern Kenya. *Phd Thesis Universite Bretagne Occidentale*, p.140.

Tiercelin, J. J., Potdevin, J., Morley, C. K., Talbot, M. R. Bellon, H., Rio, A., Le Gall, B., & Vetel, W., 2004. Hydrocarbon potential of the Meso-Cenozoic Turkana Depression, northern Kenya. I. Reservoirs: depositional environments, diagenetic characteristics, and source rock–reservoir relationships. *Marine and Petroluem Geology*, 21, pp.41–62.

Tiercelin, J., Thuo, P., Nalpas, T, Potdevin, J., 2009. Hydrocarbon Prospectivity in Mesozoic and Early Cenozoic Rift Basins in Central/Northern Kenya. *AAPG International Conference and Exihibition*, 10188, p.20.

Tiercelin, J., Thuo, P., Nalpas, T., Potdevin, J., 2009. Hydrocarbon Prospectivity in Mesozoic and Early Cenozoic Rift Basins in Central/Northern Kenya. *AAPG International Conference and Exihibition*, 10188, p.10.

Turkana-Energy, 2008. Bock 10 BB project summary. *Turkana Energy Inc.* Available at: www.turkanaenergy.com [Accessed February 27, 2012].

Vitel, W., Le Gall, B., & Johnson, C.T., 2004. Recent tectonics in the Turkana Rift (North Kenya): an integrated approach from drainage network, satellite imagery and reflection seismic analyses. *Blackwell Publishing Ltd. Basin Research*, (16), pp.165–181.

Appendix A

Digitized shots point locations of all the interpreted 5 seismic lines from Lokichar basin.

Line	Shot point	X(m)	Y(m)
TVK-13	100	3969196.326	265194.441
TVK-13	150	3971635.818	264531.863
TVK-13	200	3974045.193	263718.699
TVK-13	250	3976454.567	263026.004
TVK-13	300	3978803.708	262333.308
TVK-13	350	3981213.082	261791.199
TVK-13	400	3983652.574	261038.27
TVK-13	450	3986122.183	260375.692
TVK-13	500	3988530.026	259644.325
TVK-13	600	3993403.825	258266.947
TVK-108	100	3969838.29	262194.201
TVK-108	150	3972122.884	263021.952
TVK-108	200	3974440.587	263949.034
TVK-108	250	3976824.511	264942.335
TVK-108	300	3979109.104	265770.086
TVK-108	350	3981393.697	266697.168
TVK-108	400	3983810.731	267591.139
TVK-108	450	3986095.324	268551.33
TVK-108	500	3988479.248	269478.412
TVK-108	550	3990830.061	270405.493
TVK-108	600	3993147.765	271299.464
TVK-108	650	3995445.602	272226.278
TVK-108	692	3997432.205	272961.589
TVK-107	100	3970848.147	267604.383
TVK-107	150	3973265.181	268518.22
TVK-107	200	3975490.176	269432.058
TVK-107	250	3977794.635	270425.359
TVK-107	300	3980059.363	271259.732
TVK-107	350	3982602.214	272253.034
TVK-107	400	3984866.942	273166.871
TVK-107	450	3987267.422	274120.441
TVK-107	500	3989555.324	275034.278
TVK-107	550	3991939.248	275987.847
TVK-107	600	3994203.975	276941.417
TVK-107	650	3996624.322	277855.254

TVK-107	700	3998875.803	278550.565
TVK-107	731	4000299.535	278848.556
TVK-127	88	3983475.554	258869.701
TVK-127	100	3984270.195	259233.911
TVK-127	150	3986356.128	260227.213
TVK-127	200	3988563.244	261359.576
TVK-127	300	3993119.186	263521
TVK-127	400	3997547.986	265745.996
TVK-127	450	3999730.601	266847.898
TVK-127	429	4001086.788	267504.801
TVK-129	50	3996460.756	261427.372
TVK-129	100	3994659.569	263228.559
TVK-129	150	3992900.764	264923.794
TVK-129	200	3991141.958	266682.599
TVK-129	250	3989595.052	268738.071
TVK-129	300	3988217.678	270687.591
TVK-129	355	3986649.587	273082.109

Appendix B

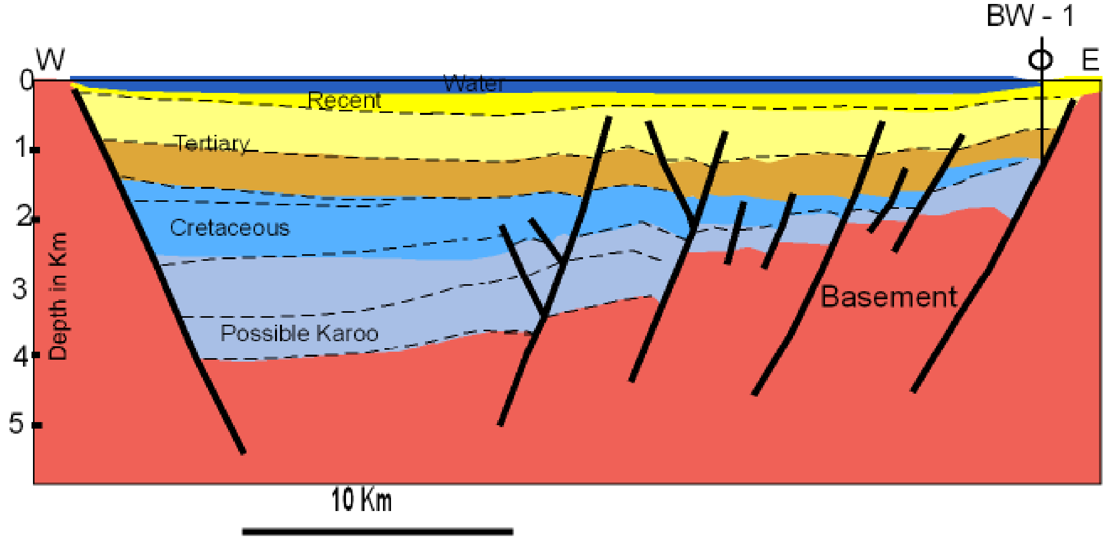

East-West structural cross-section across Albertine Graben showing positive flower structures (PEPD 2009).

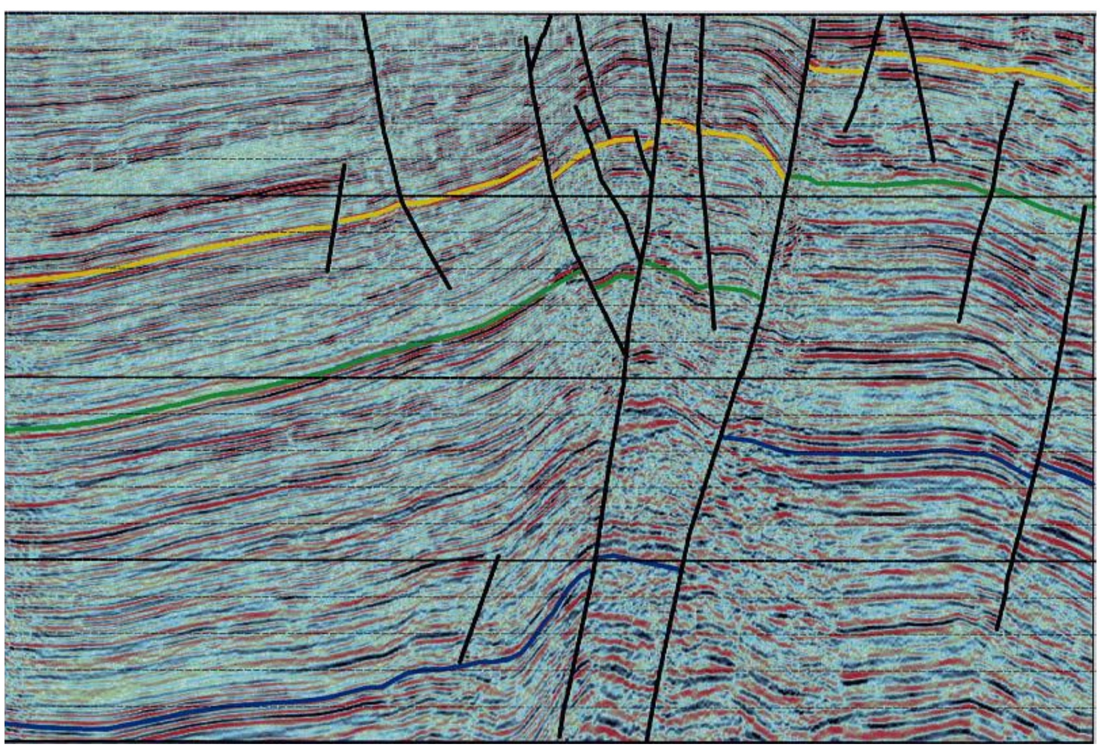

An interpretation of a positive flower structure from the seismic data of Semliki basin in the Albertine Graben (PEPD 2009).